# Complex response of dinoflagellate cyst distribution patterns to cooler early Oligocene oceans

Mark A. Woods[a], Thijs R. A. Vandenbroucke[b], Mark Williams[c], James B. Riding[a], Stijn De Schepper[d] , Koen Sabbe[e]

[a]: British Geological Survey Environmental Science Centre, Keyworth, Nottingham, NG12 5GG, UK. maw@bgs.ac.uk; jbri@bgs.ac.uk

[b]: UMR 8217 du CNRS : Géosystèmes, Université Lille 1, Avenue Paul Langevin, bâtiment SN5, 59655 Villeneuve d'Ascq Cedex, France. Thijs.Vandenbroucke@univ-lille1.fr

[c]: Department of Geology, University of Leicester, University Road, Leicester, LE1 7RH, UK. mri@leicester.ac.uk

[d]: Department of Earth Science, University of Bergen, Allégaten 41, 5007 Bergen, Norway. stijn.deschepper@geo.uib.no

[e]: Protistology and Aquatic Ecology, Department of Biology, Ghent University, Krijgslaan 281-S8, 9000 Ghent, Belgium. Koen.Sabbe@UGent.be

*: Corresponding author at: British Geological Survey Environmental Science Centre, Keyworth, Nottingham, NG12 5GG, UK. Tel.: +44 115 9363155. E-mail address: maw@bgs.ac.uk (M. A. Woods).

## Abstract

Previous studies have made extensive use of dinoflagellate cysts to reconstruct past sea surface temperature (SST). Analysis of associations of dinoflagellate cysts using

two new ocean datasets for the mid Eocene (Bartonian) and early Oligocene (Rupelian) reveals clear latitudinally constrained distributions for the Bartonian, but unexpected changes in their Rupelian distribution; a significant number of species with low and mid-latitude northern hemisphere occurrences in the Bartonian extend their northward ranges in the Rupelian, including some forms characterised as ‘warm water’ by previous studies. This suggests either that dinoflagellates are faithfully tracking a complex oceanographic response to Rupelian cooling, or that dinoflagellate sensitivity/adaptability to a range of ecological variables means that at a global scale their distributions are not primarily controlled by sea surface temperature-variability.

Previous use of dinoflagellate cysts for palaeoclimate work has relied on rather subjective and inconsistent identification of ‘warm’ and ‘cold’ water forms, rather than comprehensive analysis of community associations at the global-scale. It is clear from this study that a better understanding of the (palaeo-)ecology of dinoflagellates and their cysts is required.

Rupelian dinoflagellate cyst distribution may reflect changes in a range of environmental variables linked to early Oligocene climate-cooling, for example changes in nutrient fluxes triggered by glacially-induced base-level fall; complex reorganisation of ocean current systems between the Bartonian and Rupelian, or muted changes to Rupelian summer SSTs in the northern hemisphere that have previously been reported. Many extant dinoflagellate species also exhibit relatively broad temperature tolerance. Moreover, they have potentially extensive cryptic diversity, and are able to produce dormant cysts during short-lived environmental

deterioration, all of which may act to limit the value of undifferentiated dinoflagellate cyst assemblages for identifying climate signals.

Keywords: dinoflagellate cysts; Eocene; Oligocene; palaeoclimatology

## 1. Introduction

Previous work by Salzmann et al. (2008) and Pound et al. (2011, 2012) has established a robust database methodology (Tertiary Environments Vegetation System – TEVIS) for interpreting patterns of Cenozoic vegetation using data 'mined' from historical literature. Similarly, Vandenbroucke et al. (2010) used multivariate analysis of published occurrences of the enigmatic Chitinozoa to examine sea surface temperature (SST) relationships in the Late Ordovician. Here, we adapt the TEVIS methodology to obtain data from published literature on dinoflagellate cysts, and use them as a proxy for investigating the response of the marine realm to cooling at the Eocene – Oligocene transition. Dinoflagellates have formed a component of the microplankton in aquatic ecosystems since the Mid Triassic. They are ubiquitous in modern oceans, as well as brackish and freshwater environments, and include phototrophic, heterotrophic and mixotrophic species (Fensome et al., 1993; Jeong et al., 2010). Their fossilised organic remains (cysts) are the basis for biostratigraphical schemes (Brinkhuis and Biffi, 1993; Van Simaeys et al., 2005; Williams et al., 2004) and palaeoenvironmental analysis (Sluijs et al., 2005; Versteegh and Zonneveld, 1994). Their use to discriminate between offshore to near-shore environments (Dale, 1996; Wall et al., 1977) has made them invaluable for the identification of different systems tracts in sequence stratigraphy (Brinkhuis, 1994; Sluijs et al., 2005), and the

apparent strong relationship between the global distribution of extant marine dinoflagellates and SST (e.g. Marret and Zonneveld, 2003; Zonneveld et al., 2013) has formed the basis of their widespread use in palaeoclimate reconstruction and tracking palaeoclimate oscillations (Brinkhuis and Biffi, 1993; Brinkhuis et al., 1998; Esper and Zonneveld, 2007; Masure and Vrielynck, 2009; Mudie et al., 2001; Sluijs et al., 2005; Wall et al., 1977).

This work reconstructs global distributions of dinoflagellate cysts between a warmer mid Eocene (Bartonian) Earth and a cooler early Oligocene (Rupelian) Earth, and uses multivariate analysis and range data to investigate the extent to which these patterns are significant for understanding the pattern of ocean temperature change across the Eocene – Oligocene boundary. We also explore how our results might reveal potential weaknesses in the ability of dinoflagellate cysts to track global climate change. We examine the hypothesis that at a global scale, dinoflagellate cyst latitudinal distributions shifted equatorward from the late mid Eocene to the early Oligocene in response to climate cooling. Published data on planktonic foraminifera in Tanzania, showing a major faunal turnover and size reduction of individual species at the Eocene/Oligocene boundary, suggests that even the modest SST reductions at low latitudes had a significant impact on marine habitats (Wade and Pearson, 2008), and a strong biotic signal in dinoflagellate cyst data from this time interval might therefore be anticipated. Previous studies using dinoflagellate cysts to track Eocene and/or Oligocene climate change (e.g. Bijl et al., 2011; Brinkhuis, 1994; Brinkhuis and Biffi, 1993; Guerstein et al., 2008) have tended to focus on relatively limited geographical areas, rather than adopting a methodology to track ocean-wide species responses across this time interval.

## 2. Background

A transition in global climate state began in the latest Eocene (Wade et al., 2012), probably triggered by a reduction in atmospheric $CO_2$ below a critical threshold (Anderson et al., 2011; DeConto and Pollard, 2003; Pagani et al., 2011; Pearson et al., 2009). It culminated in the establishment of the East Antarctic Ice Sheet associated with further cooling in the early Oligocene, termed Oi-1. The widely recognised early Oligocene cooling event (Eldrett et al., 2009; Liu et al., 2009; Wei, 1991) lasted about 400,000 years, and is dated to about 34 Ma (Fig. 1).

In the mid Eocene, annual mean SSTs ranged from c. 35°C at the equator to 15 to >20 °C at high latitudes (Bijl et al., 2009). Corresponding values for the early Oligocene were reduced by about 5°C at mid to high latitudes, with smaller temperature reductions in tropical and equatorial regions (Liu et al., 2009). Oxygen isotope data from benthic foraminifera show that the Bartonian was a relatively warm and stable climatic interval compared to the relatively cooler Rupelian (Fig. 1). Apart from a transient warming event at 40 Ma (Bohaty et al., 2009), termed the Middle Eocene Climate Optimum (Bohaty and Zachos, 2003), temperatures in the Bartonian mostly show a gradual fall from their peak in the late Paleocene and early Eocene (Bijl et al., 2009). Imprinted on this overall trend are higher frequency cycles of orbitally-driven climate change that variably affected SST values (Sloan and Huber, 2001; Burgess et al., 2008; Pälike et al., 2006; Wade and Pälike, 2004), as well as larger regional temperature oscillations in SST, of perhaps 10°C, that have been reported in the uppermost middle Eocene (presumably Bartonian) of the subtropical western North Atlantic (Wade and Kroon, 2002). However, none of these fluctuations are inferred to

have had a sustained impact on marine ecology. In the lower and middle Eocene, coccolithophores exhibit maximum species richness for the Paleogene (Bown et al., 2004), and data from Eocene benthonic foraminifera suggests relatively stable phyletic composition (Less and Özcan, 2012). As remarked by MacLeod et al. (2000), middle Eocene planktonic foraminifera from low and mid-latitudes show a broad and fairly uniform distribution of morphotypes, with almost constant relative abundance between zones P9 (Ypresian) and P14 (Bartonian) (Fig. 2); significant changes in both Paleogene planktonic foraminifera (MacLeod et al., 2000) and coccolithophores (Bown et al., 2004) coincided with major climate-change events, including the Eocene – Oligocene transition.

## 3. Material

Two stratigraphically well-defined time slabs were selected for dinoflagellate cyst analysis; the Bartonian (late mid Eocene; 41.2 – 37.8 Ma) and Rupelian (early Oligocene; 33.9 – 28.1 Ma) (Figs 2, 3). Time slabs were chosen for optimum potential for climate contrast between them, whilst minimising both temporal separation and the influence of transient climate effects within them. The Priabonian (latest Eocene) is less attractive for investigation. It straddles the onset of the climate cooling event that extends into the Rupelian (Houben et al., 2012), but variable quality of stratigraphical data in published accounts means that accurate and consistent interpretation of the dinoflagellate cyst record with respect to the cooling event would be problematic, or would require a subjective interpretation to be imposed. Literature records of dinoflagellate cysts in Bartonian and Rupelian successions were used to construct two new global datasets of taxa present within these time slabs at

different localities. These datasets contain species (presence/absence) and location data, chronostratigraphical, biostratigraphical, lithostratigraphical and palaeoenvironmental information. Raw data were obtained by searches of digital reference indexes, institutional library catalogues, and thematic literature collections, the latter particularly including the global palynological reference collection assembled by John Williams at the Natural History Museum (London). Potential limitation of Rupelian data as a consequence of sea level fall associated with early Oligocene glaciation of Antarctica is not reflected by the relative sizes of our two datasets, although it may potentially affect its relative completeness in particular palaeoenvironments.

*Dating: chronostratigraphy, biostratigraphy, magnetostratigraphy*

Geochronometric, biostratigraphical (dinoflagellate cyst, planktonic foraminifera, calcareous nannofossil) and magnetostratigraphical criteria are used to recognise the Bartonian and Rupelian. These stratigraphical criteria are summarised in Figures 2 and 3. Confidence of assignment to a particular time slab is based on assessment of published stratigraphical data (1 = high confidence; 3 = low confidence), and this is indicated in a separate field in the data compilation (see Supplementary Data). Brinkhuis and Biffi (1993) noted that long-range biostratigraphical correlation using dinoflagellate cysts is problematic because of the effects of provincialism and palaeoenvironment, and this may affect the confidence of age assignment of sites where dinoflagellate cysts alone are the basis of age diagnosis. Generally, sites dated with low confidence are those that are likely to contain at least parts of chronostratigraphical intervals adjacent to either the Bartonian or Rupelian. Nevertheless, in all these cases their dinoflagellate cyst floras are highly likely to span

the time slabs critical to this investigation; other sites that potentially include the Bartonian or Rupelian, but for which confirmatory stratigraphical data were scant, were excluded from this study. In some cases age confidence was enhanced by omitting sample data from parts of successions where dating evidence was much less certain.

*Location*

Location data are recorded as longitude and latitude, either directly transcribed from the relevant publication, or derived from Google Earth™ using published geographical details. Where the quality of published data precludes a precise location fix, then a site is defined by a radius from a designated point. All modern longitude and latitude data for sites were converted to values relevant to the Bartonian or Rupelian (Fig. 4C, D) using PALEOMAP PointTracker software for global palaeogeography reconstructions at 40 Ma (early Bartonian) and 30 Ma (mid Rupelian).

*Lithostratigraphy and palaeoenvironment*

Where available, lithostratigraphical and palaeoenvironmental information has been included in the datasets. Together, these data provide an indication of how nearshore or basinal a succession is likely to be, and are a guide to the likely influence of local palaeogeographical factors on dinoflagellate cyst composition.

*Dinoflagellate cyst data, taxonomy and nomenclature*

Following the rationale used to build the Cenozoic vegetation databases using TEVIS (Salzmann et al., 2008; Pound et al., 2011, 2012), there is minimal reinterpretation of the primary published data, which in this study represents the dedicated work of dinoflagellate specialists. This is an essential feature of our methodology, which permits rapid construction of global-scale databases, focusing on large-scale trends that are beyond the scope of individual studies. The sheer quantity of data assembled, and the broad-scale of the analysis, militate against problems caused by variable taxonomic interpretation in source literature used to build the databases. There are obvious practical problems in attempting to directly re-interpret such large volumes of data. Extensive indirect re-interpretation of published records is also undesirable, because strict application of current understanding of taxonomic and range concepts is likely to falsely eliminate data that represent genuine records of taxa that were previously differently interpreted.

Notwithstanding the above, some limited screening of taxonomic nomenclature has been applied where this is clearly beneficial for data analysis, including removal of obvious species synonyms. In a few cases, where clear doubt existed about species records, these were checked against any associated published figures/plates, or the records deleted. Only taxa identified to species-level are included in the datasets; identifications qualified by “?” and “cf.” are regarded as definite for the purposes of the statistical analyses, but records qualified by “aff.” are excluded. No informal nomenclature, prevalent in some older publications, has been included, but data fields describing the higher taxonomic classification of species have been added. An important consequence of the methodology adopted in this study is that the species

names appearing in our dataset largely reflect understanding of dinoflagellate cyst taxonomy at the time of publication. Current species concepts, and the stratigraphical ranges of taxa, may be broader or narrower than those appearing in historical literature.

Potential distortion of ecological conclusions based on this methodology can arise where there is reworking of dinoflagellate cysts, either through erosion of pre-existing rock successions, or by pre-burial lateral transport of dinoflagellate cysts within sedimentary basins. Reworked taxa, identified in published source data for this study (e.g. De Coninck, 1986; Frith, 1996; Heilmann-Clausen and Van Simaeys, 2005; Jaramillo and Oboh-Ikuenobe, 1999; McMahon, 1997; Schiøler, 2005) or inferred from known range data, were excluded from the analysis. The possibility that some reworked taxa form part of our analysis cannot be excluded. However, the large quantity of data analysed in this study coupled with evidence of limited reworking of dinoflagellate cysts in younger sediments (Mertens et al., 2009; Verleye and Louwye, 2010), suggest that this factor is unlikely to bias our results. Mertens et al. (2009) reported that reworking affected a maximum of 7% of the cysts recorded in Quaternary sediments at four widely distributed sites, and statistical analysis of shelf to basin transects in the south-east Pacific found negligible evidence of lateral transport of cysts, including by near-shore and bottom water currents (Verleye and Louwye, 2010).

The datasets contain presence/absence data for dinoflagellate cysts from 71 Bartonian sites and 123 Rupelian sites (Fig. 4; Appendix 1A). Figure 4 shows that there is a general paucity of low latitude and southern hemisphere data for each time interval,

but in the northern hemisphere data coverage is good. A total of 460 taxa are represented in the Bartonian dataset, and 492 taxa in the Rupelian dataset, with 268 taxa occurring in both time slabs, representing more than 50% of the taxa in each individual time slab. Information about relative species abundance in samples was collected or derived where possible, but inconsistency in the quality of these data precluded their use in statistical analyses. Similar problems with abundance data were encountered by Masure and Vrielynck (2009) in their global analysis of Upper Albian dinoflagellate cysts. The large percentage of taxa shared by the Bartonian and Rupelian is reflected in the global plot of dinoflagellate generic diversity across the Eocene – Oligocene boundary, which is almost flat (MacRae et al., 1996).

Assessments of individual localities show that, despite the range of palaeoenvironments represented in this study, many Bartonian and Rupelian sites have more than 70% of taxa common to both time slabs; localities with a lower proportion of shared taxa tend to occur at higher palaeolatitudes. The high percentage of shared taxa between the time slabs mitigates the impact of biological factors (e.g. evolutionary change) on the interpretation of our results.

Copies of all the datasets, and the references from which they were compiled, are provided as Supplementary Data. The author citations, with the relevant bibliographical references, of all the dinoflagellate cyst taxa at and below generic level which are quoted in this contribution and associated Supplementary Data can be found in Fensome and Williams (2004), or online at: http://dinoflaj.smu.ca/~macrae/pdf/dinoflaj.pdf.

## 4. Method

We used ordination techniques to study relationships between sample sites on the basis of their full dinoflagellate cyst composition (presence/absence data). Ordination techniques allow visualisation of large datasets in low-dimensional (usually two-dimensional) ordination diagrams, in which the ordination axes represent the most important gradients in species composition (Jongman et al. 1995). These can then be related to known environmental variation, i.e. palaeolatitude, depositional basin (North Sea, Arctic, Atlantic, Tethys, Indian and Pacific Ocean) and palaeoenvironment (position of sites with respect to the shore, i.e. inshore vs. offshore). Multivariate analysis has previously been used by Versteegh and Zonneveld (1994), Marret and Zonneveld (2003), Esper and Zonneveld (2007), and Zonneveld et al. (2013) to investigate the relationship between dinoflagellate cyst distribution and environmental parameters.

Three primary datasets have been investigated: (1) a Bartonian dataset comprising 460 species and 71 sites, (2) a Rupelian dataset with 492 species and 123 sites, and (3) a combined dataset comprising only those species that occurred in both time slabs (268 species and 175 sites). Analysis of the latter dataset allowed comparison of potential latitudinal shifts in species distributions between the Bartonian and Rupelian sites. All ordination analyses were performed using the program CANOCO for Windows 4.5 (ter Braak and Smilauer 1998). To aid the analysis of particular variables other than latitudinal position, key features of the primary data (for example, ocean basin, inshore/offshore palaeoenvironment) were introduced as qualitative (dummy) variables (cf. ter Braak and Smilauer, 1998).

Preliminary Detrended Correspondence Analyses (DCA) revealed strong turnover in species composition between the samples in all datasets investigated ('length of gradient' > 4), indicating that unimodal ordination techniques were the most appropriate for all analyses (Jongman et al., 1995). DCA was used instead of Correspondence Analysis (CA) to eliminate the arch effects in the analyses (ter Braak and Smilauer 1998). Analyses were initially performed on datasets (1) and (2) (Figs 5 and 6); subsequently the data were 'filtered' by removing groups of samples from further analyses, in order to eliminate confounding basin-specific effects (provincialism) (see Supplementary Data: Suppl. Figs 1 and 2). In a final analysis of the combined Bartonian and Rupelian data (dataset (3), Fig. 7), a further data reduction (sample elimination) was performed in order to minimise basin-specific and potential palaeoenvironmental effects. In this last analysis, the Bartonian samples were active (i.e. the DCA was only based on these samples) and the Rupelian samples were supplementary (i.e. they were passively plotted in the Bartonian DCA, only on the basis of their resemblance in dinoflagellate cyst composition to the Bartonian samples).

To further understand the changes in the global distribution of dinoflagellate cyst taxa that are common to both time slabs, simplified latitudinal range plots (using 5° bins; see Supplementary Data: Latitudinal Ranges) were generated for all species in dataset (3), and global occurrence maps plotted for selected species. These distributions, plotted using corrected palaeolatitudes on modern geographical base maps, are shown in Figure 8. Taxa were selected on the basis of having been consistently designated as 'temperature sensitive' in previous studies (Table 1). Opinion is divided about the

temperature sensitivity of some dinoflagellate cysts (Table 1), and the present study is open-minded about the significance of the plots we illustrate for understanding SST.

## 5. Results

DCA of the global Bartonian and Rupelian datasets shows that southern hemisphere communities are clearly different from northern hemisphere communities in both time slabs (Fig. 5; see **7**). Because latitudinal coverage of sample sites is poor in the southern hemisphere, we decided to restrict further ordination analyses to the northern hemisphere sites.

After omitting the 14 southern hemisphere samples and two outlier samples (B57 and B58), we performed DCA on the remaining northern hemisphere Bartonian data (365 species, 55 samples). Along the first axis, sites are separated on the basis of their palaeolatitudinal position, with low latitude samples (from three separate basins: Atlantic, Indian and Pacific oceans) on the right side of the first axis, high latitude samples on the left side, and samples from intermediate latitudes (50 – 30° N) occupying a somewhat intermediate position (Fig. 6B). The latitudinal gradient in cyst composition appears to be mainly driven by the low latitude samples, with high latitude samples (80 – 60˚ N) having a species composition that is more-or-less similar to samples from the many mid-latitude sites. As well as a latitudinal signal, we can also distinguish a clear 'basin-effect', with sites in the North Sea and the palaeo-Tethys Ocean being more or less separated along the second axis (Fig. 6A).

In contrast with the Bartonian dataset, DCA of the northern hemisphere Rupelian data (449 species and 106 sites, after omitting 15 southern hemisphere samples and the

outliers R41 and R77) revealed no distinct latitudinal trend in species composition. The Pacific sites are separated from most other samples which form a tight cluster on the right side of the first ordination axis (Figs. 6C, D). The single (Indian Ocean) sample from the 10 – 0° N latitude class does not appear to be very different from the other samples, nor do the samples from the 30 – 20° N class (Fig. 6D). Basin specificity is also less pronounced (except for the Pacific samples), although Atlantic and North Sea samples do seem to be separated along the second axis (Fig. 6C). It is likely that a general lack of tropical samples (only one sample after omission of outliers R77 (Nigeria) and R41 (Indian Ocean)) is at least partly responsible for the absence of a latitudinal trend in the Rupelian dataset, with most samples being located between 45 – 65 °N.

To get a clearer insight into any underlying latitudinal control on the Bartonian and Rupelian data, basin-specific effects were initially reduced by confining analyses to samples from the palaeo-North Sea, Atlantic and Arctic oceans; basins for which palaeogeographical data suggest few barriers to North – South migration during the Eocene – Oligocene transition. However, these results appear to show the persistent influence of basin-setting and inshore to offshore environmental gradients (Suppl. Fig. 1), predominantly caused by the inclusion of samples from the palaeo-North Sea region which are predominantly ‘inshore’. Therefore, in a final analysis of the combined Bartonian and Rupelian dataset (dataset (3)), residual basin-effects and palaeoenvironmental influences were minimised by removing the North Sea samples (Fig. 7). As the latitudinal signal was strongest in the Bartonian dataset (cf. Fig. 6A), we used the 15 remaining (Atlantic and Arctic) Bartonian samples as active samples, thus providing a (latitudinal) scaffold onto which the Rupelian samples are plotted as

supplementary (‘passive’) samples. The underlying idea is that if, as hypothesized, dinoflagellate communities shift southward in a cooler climate, Rupelian communities from a specific latitudinal belt would become more similar to Bartonian communities from a higher latitudinal belt, since in a warmer period the same communities would be found at higher latitudes. Surprisingly, there is no evidence supporting this hypothesis at the community level. On the contrary, Fig. 7 clearly shows that Rupelian high latitude communities (60 – 80 °N) appear to become more similar to mid-latitude (30 – 60 °N) Bartonian samples. While as a result of the stringent data reduction, the number of samples included in the analysis is rather low, and some latitudinal belts (20 – 30, 40 – 50, 50 – 60 °N) are poorly or not represented in the Bartonian latitudinal scaffold, the signal from the Rupelian high northern latitudinal samples is clear: we find little evidence for a southward shift of dinoflagellate communities from the Bartonian to the Rupelian.

Examination of latitudinal range plots of taxa that are common to both time slabs (see Supplementary Data: Latitudinal Ranges), as well as the distributions of some ‘temperature sensitive’ taxa, also suggest lack of a clear cooling signal in Rupelian dinoflagellate cyst data. Latitudinal range plots for all taxa occurring in both the Bartonian and Rupelian reveals three predomimant patterns (Appendix 1B): 1) taxa showing negligible change in their most northerly limit in the northern hemisphere; 2) taxa with a lower northern latitudinal limit in the northern hemisphere in the Rupelian compared to the Bartonian; 3) taxa extending their northern latitudinal limit in the northern hemisphere in the Rupelian compared to the Bartonian. Numbers of species in categories (1) and (3) significantly exceed those in category (2), and category (3) is the largest (Appendix 1B). Amongst the taxa previously interpreted as temperature-

sensitive, some warm/cold-water forms exhibit trends consistent with Rupelian cooling, such as the southward movements of 'warm-water' *Deflandrea arcuata* (Fig. 8C) and 'cold-water' *Rottnestia borussica* (Fig 8F) and *Svalbardella cooksoniae* (Fig. 8B). Other taxa suggest the opposite trend, with persistence or northward extension of the Rupelian ranges of 'warm-water' forms (e.g. *Tectatodinium pellitum*, *Lingulodinium machaerophorum*; Fig. 8A, D). *Polysphaeridium zoharyi*, regarded as a tropical to subtropical indicator species in modern oceans (Marret and Zonneveld, 2003; Zonneveld et al., 2013), extends from equatorial and subtropical latitudes in the Bartonian to high mid-latitudes in the Rupelian (Fig. 8E). The plot for the Rupelian occurrence of all selected warm-water indicator species shows a local concentration immediately south of Australia (Fig. 9B), and published data for this region suggests a persistent warm-water influence from the Late Eocene to Quaternary (Brinkhuis et al., 2004). Overall, between the Bartonian and Rupelian there appears to be negligible change in the global distributions of all cold-water/high-latitude and warm-water/low-latitude taxa (Fig. 9). An important caveat concerning these trends is that they are also affected by lack of data rather than purely reflecting a palaeoecological response. However, the consistency of these trends across significant numbers of taxa suggests that data-paucity alone is insufficient to explain them.

## 6. Interpretation

The starting hypothesis for this paper was that, based on previous use of dinoflagellate cysts in palaeoclimate work (Brinkhuis and Biffi, 1993; Brinkhuis et al., 1998; Esper and Zonneveld, 2007; Masure and Vrielynck, 2009; Mudie et al., 2001; Sluijs et al., 2005; Wall et al., 1977), and on current understanding of extant dinoflagellate

distributions (Marret and Zonneveld, 2003; Zonneveld et al., 2013): 1) dinoflagellate cyst assemblages as a whole would robustly track global climate change at the Eocene – Oligocene transition; 2) there would be a well established palaeolatitudial gradient of dinoflagellate cyst taxa in both the Bartonian and Rupelian; 3) that the effect of global cooling in the latest Eocene and early Oligocene would be manifest as a steepening of this palaeolatidudinal gradient, and that this would be accompanied by significant equator-ward movement of taxa that are present in both time slabs. Our analysis of dinoflagellate cyst data actually reveals more complex patterns that may reflect a more complex oceanography, or suggests that across the Eocene – Oligocene transition the predominant control on dinoflagellate cyst distributions may not be SST. There is a relatively well-defined palaeolatitudinal gradient in northern hemisphere data for the Bartonian. Low latitude sites have a distinct dinoflagellate cyst composition whilst high and mid-latitude cyst taxa are more similar, suggesting a weak thermal gradient. In contrast, there is no clear latitudinal gradient in northern hemisphere Rupelian data. Partly this reflects lack of low-latitude data points (a single site, R77), but it is also consistent with latitudinal range data that suggest both northward and southward movement of a significant number of taxa in the northern hemisphere in the Rupelian (Appendix 1B).

## 7. Discussion

Zonneveld et al. (2013) determined that latitudinal gradient was the most important influence on their dataset of modern dinoflagellates, and that SST, phosphate and nitrate concentrations are the most significant environmental variables that can be related to modern distribution patterns. In this context, it is striking that both

community-level analysis of the northern hemisphere dinoflagellate cyst assemblages (i.e. DCA results) and latitudinal range plots identify apparently paradoxical palaeolatitudinal range shifts of taxa between the Bartonian and Rupelian. These unexpected results may, in part, be explained by the uneven global coverage of our dataset as well as methodological limitations; they may also reflect complex changes in oceanography (for example patterns of warm and cool currents) that confuses the global relationship of dinoflagellate cysts to palaeolatitude, or show that ecological tolerance/adaptability of dinoflagellate cysts caused SST to be subordinate to other factors in controlling their net latitudinal distribution in the Rupelian.

### *7.1. Data coverage, methodological assumptions and limitations*

Our methodology assumes that the time intervals (slabs) we have analysed are broadly representative of two different global climatic states, one warm (Bartonian) and one cool (Rupelian). For each time interval we assume that the contained taxa have consistent ecology, have not been significantly affected by re-working (**4** *above*), and that orbitally driven patterns of climate change within each have had less impact on the global distributions of taxa than the climate change events that occur between the time intervals (MacLeod et al., 2000; Less and Özcan, 2012). Finally, because of historical and on-going revisions to the definition of the selected time intervals, it is possible that there is some error in how stratigraphical successions have been assigned to time intervals, although this is partly addressed by assigning confidence levels to stratigraphical assignments in our datsets. The degree to which the above assumptions are not fully met will affect the fidelity of our results and interpretations, and may explain in part why we have difficulty in discerning a clear latitudinal signal from the Rupelian data.

In mitigation, our methodology outlines procedures and describes published evidence that seeks to reduce or acceptably quantify the adverse potential impact of our inherent assumptions. Also, the large size of both datasets helps to reduce the statistical effect of individual sites that strongly depart from our ideal criteria; data classes for age precision, depositional basin and environment allow statistical filtering of potentially problematic data. Any residual bias in our data might be expected to equally affect both Bartonian and Rupelian datasets, but whilst data for the Bartonian yield a good latitudinal signal, a reliable signal for the Rupelian (the larger of the two datasets) is not detectable.

### *7.2. Oceanography*

Pole-ward range shifts of Rupelian dinoflagellate cysts in the northern hemisphere may suggest that aspects of environmental change related to Eocene – Oligocene cooling modulated the response of dinoflagellate cysts to this event, compared to the much more direct impact reported for planktonic foraminifera and calcareous nannofossils (Wade and Pearson, 2008; Wei, 1991). Alternatively, the complex response patterns of Rupelian dinoflagellates might reflect their sensitivity to local patterns of marine circulation with different temperature profiles. In both central Italy and the Southern Ocean, the sensitivity of dinoflagellate cysts to warm ocean currents has been detected (Brinkhuis and Biffi, 1993; Brinkhuis et al., 2004). This has produced low-latitude dinoflagellate cyst associations in Eocene – Quaternary successions off the coast of Tasmania (palaeolatitude 59°S) (Brinkhuis et al., 2004), and in Italy, warm and cool phase dinoflagellate cyst associations in Eocene – Oligocene strata (Brinkhuis and Biffi, 1993) may reflect the intermittent influence of

the Subtropical Neotethys Current (STENT) (Jovane et al., 2009). Warm ocean currents may also be the cause of inexplicably high SSTs at mid to high latitudes in the late Eocene and early Oligocene of the northern hemisphere (Liu et al., 2009), and explain some of the unexpected results of our study.

### *7.3. Nutrient regime*

Although the distribution of modern organic walled dinoflagellate cysts is predominantly related to SST and latitude, the next biggest controls are salinity and nutrients (Zonneveld et al., 2013), which to a greater or lesser degree reflect the offshore to onshore gradient (Marret and Zonneveld, 2003). It is therefore likely that related environmental changes to global cooling at the Eocene – Oligocene boundary could have an impact on the results of our study.

A modelled c. 70 m fall in sea level is associated with early Oligocene cooling and the onset of Antarctic glaciation (Coxall et al., 2005), and both palaeontological and sedimentological data (Alegret et al., 2008; Brinkhuis and Biffi, 1993; Śliwińska et al., 2010) show that this time coincides with enhanced riverine input of eroded sediments into marine basins. The effects of enhanced nutrient delivery to the marine realm would be amplified across flooded continental shelves and enclosed basins; palaeogeographical settings that are strongly represented in our northern hemisphere data for the Rupelian. In the North Sea, this fall in sea level produced prograding muddy and sandy sediments derived from Fennoscandia, overlying Eocene hemipelagic clays (Śliwińska et al., 2010). Elsewhere, contemporary tectonism combined with eustatic sea level fall radically altered the nature and volumes of sediment entering marine basins, for example in the Mediterranean (Brinkhuis and

Biffi, 1993) and off the coast of southern Spain, where foraminifera provide evidence for increases in nutrient fluxes to deep marine early Rupelian settings (Alegret et al., 2008). This, and the lack of DCA evidence for equator-ward movement of Rupelian dinoflagellate cysts from predominantly open-ocean sites, suggests that any changes in the nutrient regime of the marine realm in the Rupelian may not have been limited to shelfal regions.

The importance of nutrients in driving the evolution of the dinoflagellates is exemplified by the distinct character of southern hemisphere Eocene – Oligocene dinoflagellate cysts. These high southern latitude dinoflagellates developed their endemic character ('Transantarctic Flora') in the early mid Eocene (Bijl et al., 2011), initially in response to increases in ocean fertility, but probably later became modulated by reductions in SST (Bijl et al., 2011). Mathematical 'decision-making' models also reveal the influence of light and nutrients on the diurnal movements of modern dinoflagellates, suggesting that changes in the relative balances of these two variables can trigger different responses (Yamazaki and Kamykowski, 2000). This raises the possibility that at least part of the distribution of dinoflagellate taxa in the Rupelian is the result of an ecological trade-off between several simultaneously varying factors that are important for dinoflagellate well-being.

### *7.4. Ecological tolerance and adaptability*

Data from our study, particularly the large percentage of shared taxa between the Bartonian and Rupelian and the apparent pole-ward Rupelian migration of many dinoflagellate cyst species in the northern hemisphere, suggests that dinoflagellate cyst taxa are relatively robust to environmental change. This may partly reflect the

548 astonishing cryptic diversity recently discovered in extant dinoflagellates (Stern et al.,
549 2010; Murray et al., 2012). Broad temperature tolerance is also suggested by
550 comparison of Pliocene dinoflagellate cysts with analytically determined temperature
551 measurements (De Schepper et al., 2011); the SST range of many dinoflagellate cyst
552 taxa is large compared to the average cooling of 5.4°C (polar regions; Liu et al., 2009)
553 to 2.5°C (tropical regions; Lear et al., 2008) at the Eocene – Oligocene transition.
554 Unlocking the SST signal from dinoflagellate cyst data may ultimately depend on
555 analysis of their abundance (De Schepper et al., 2011), although challenges exist to
556 applying this methodology at a global scale across numerous sites. In a quantitative
557 analaysis of dinoflagellate cysts to track Eocene – Oligocene climate change in central
558 Italy, Houben et al. (2012) were careful to select particular 'warm' or 'cool' oceanic
559 taxa, aware that inclusion of all taxa could create unwanted 'noise'.
560
561 Investigation of high-latitude northern hemisphere climate at the Eocene – Oligocene
562 transition suggests a complex response to cooling, with limited ice growth (Peck et
563 al., 2010) and extreme seasonality; modelled climate simulations suggest very cold
564 winters contrasting with warm summers with high precipitation (Eldrett et al., 2009).
565 This climate response in the northern hemisphere could help explain why our
566 Rupelian data (overwhelmingly concentrated in the northern hemisphere) do not show
567 a dominant latitudinal effect. Cyst formation could also have mitigated the effects of
568 seasonally adverse conditions (Dale, 1983; Matsuoka and Fukyo, 2000; Sarjeant et al.,
569 1987), and may partly explain why diversity plots of dinoflagellate cysts show only a
570 small drop between the Ypresian/Bartonian and Rupelian (MacRae et al., 1996).
571
572

## 8. Conclusions

This study has sought to investigate Eocene – Oligocene climate change using published data on the occurrence of dinoflagellate cysts; to understand the pattern of change in distribution between the Bartonian and Rupelian; the extent to which this distribution is likely to faithfully track changes in SST, and the implications this has for understanding the consequences of early Oligocene global cooling; the extent to which these distributions are likely to be unrelated to changes in SST, and the consequences for use of dinoflagellate cyst data in palaeoclimate work.

Our results suggest the following:

1) Global distributions of dinoflagellate cysts in the Bartonian show a good latitudinal relationship and suggest a weak thermal gradient, in agreement with global SST estimates for this time interval (Bijl et al., 2009). This suggests that our methodology is reliable, and our assumptions and data coverage acceptable.

2) Rupelian dinoflagellate cyst distributions do not show a clear relationship to latitude. Statistical analyses and range data suggest that mid- to high-latitude dinoflagellate cyst associations in the cooler Rupelian are more like lower latitude associations in the globally warmer Bartonian.

3) It is possible that at least part of the Rupelian dinoflagellate cyst distribution reflects latitudinally discordant influences on SST, such as warm ocean currents (Brinkhuis et al., 2004), or perhaps unusual northern hemisphere seasonality that maintained relatively high summer temperatures at high latitudes (Eldrett et al., 2009).

4) To some extent, the distributions of dinoflagellate cysts in the Rupelian may be significantly influenced by factors other than SST, potentially complicating how their distributions are interpreted with respect to climate change events. The factors affecting dinoflagellate cyst distribution in the Rupelian may be connected to related environmental changes associated with Rupelian cooling, such as sea level fall associated with the onset of Antarctic glaciation. Studies of Pliocene and extant dinoflagellates also suggest that many have broad temperature ranges (De Schepper et al., 2011) and high genetic diversity (Stern et al., 2010; Murray et al., 2012); whilst dinoflagellate cysts appear to have optimised distributions to SST in the Bartonian, their biology may have allowed greater flexibility of response to Rupelian climate change. Our work highlights the need for better understanding of the biology and (palaeo-) ecology of dinoflagellates, and how this affects their response to changes in key environmental parameters and governs their distribution in present and past oceans.

**ACKNOWLEDGEMENTS**

This research was supported by the BGS Climate Change Research Programme directed by Dr Michael A. Ellis. We are grateful to Emily Peckover (University of Leicester) for assisting with data compilation, and to Stewart G. Molyneux and Ian P. Wilkinson (British Geological Survey) for early reviews of this manuscript. MAW and JBR publish with the permission of the Executive Director, British Geological Survey (NERC). TRAV acknowledges financial support from the French “Agence Nationale de la Recherche” through grant ANR-12-BS06-0014 “SeqStrat-Ice”.

## REFERENCES


Alegret, L., Cruz, L. E., Fenero, R., Molina, E., Ortiz, S., Thomas, E., 2008. Effects of the Oligocene climatic events on the foraminiferal record from Fuente Caldera section (Spain, western Tethys). Palaeogeography, Palaeoclimatology, Palaeoecology 269: 94 – 102.

Anderson, J. B., Warny, S., Askin, R. A., Wellner, J. S., Bohaty, S. M., Kirshner, A. E., Livsey, D. N., Simms, A. R., Smith, T. R., Ehrmann, W., Lawver, L. A., Barbeau, D., Wise, S. W., Kulhenek, D. K., Weaver, F. M., Majewski, W., 2011. Progressive Cenozoic cooling and the demise of Antarctica's last refugium. PNAS 108: 11356 – 11360.

Bijl, P. K., Pross, J., Warnaar, J., Stickley, C. E., Huber, M., Guerstein, R., Houben, A. J. P., Sluijs, A., Visscher, H., Brinkhuis, H., 2011. Environmental forcings of Paleogene Southern Ocean dinoflagellate biogeography. Paleoceanography 26: PA1202.

Bijl, P. K., Schouten, S., Sluijs, A., Reichart, G.-J., Zachos, J. C., Brinkhuis, H., 2009. Early Palaeogene temperature evolution of the southwest Pacific Ocean. Nature 461: 776 – 779.

Bohaty, S. M., Zachos, J. C., 2003. Significant Southern Ocean warming event in the late middle Eocene. Geology 31: 1017 – 1020.

Bohaty, S. M., Zachos, J. C., Florindo, F., and Delaney, M. L., 2009. Coupled greenhouse warming and deep-sea acidification in the middle Eocene. Paleoceanography 24: PA2207.

Bown, P. R., Lees, J. A., Young, R., 2004. Calcareous nannoplankton evolution and diversity through time. In: Thierstein, H. R., Young, J. R. (Editors), Coccolithophores: from molecular processes to global impact. Springer-Verlag, Berlin, pp. 481 – 508.

Brinkhuis, H., 1994. Late Eocene to Early Oligocene dinoflagellate cysts from the Priabonian type-area (Northeast Italy): biostratigraphy and paleoenvironmental interpretation. Palaeogeography, Palaeoclimatology, Palaeoecology 107: 121 – 163.

Brinkhuis, H., Biffi, U., 1993. Dinoflagellate cyst stratigraphy of the Eocene/ Oligocene transition in central Italy. Marine Micropalaeontology 22: 131 – 183.

Brinkhuis, H., Bujak, J. P., Smit, J., Versteegh, G. J. M., Visscher, H., 1998. Dinoflagellate-based sea surface temperature reconstructions across the Cretaceous – Tertiary boundary. Palaeogeography, Palaeoclimatology, Palaeoecology 141: 67 – 83.

Brinkhuis, H, Munsterman, D. K., Sengers, S., Sluijs, A., Warnaar, J, Williams, G. L., 2004. Late Eocene– Quaternary dinoflagellate cysts from ODP Site 1168, off

western Tasmania. In: Exon, N.F., Kennett, J.P., Malone, M.J. (Eds.), Proceedings of the Ocean Drilling Program, Scientific Results 189: 1 – 36 [CD-ROM].

Burgess, C. E., Pearson, P. N., Lear, C. H., Morgans, H. E. G., Handley, L., Pancost, R. D., Schouten, S., 2008. Middle Eocene climate cyclicity in the southern Pacific: Implications for global ice volume. Geology 36: 651 – 654.

Costa, L. I., Manum, S. B., 1988. The description of the interregional zonation of the Paleogene (D1-D15) and the Miocene (D16-D20). In: Vinken, R. (Editor), The Northwest European Tertiary Basin. Results of the International Geological Correlation Programme. Project No. 124. Geologisches Jahrbuch 100: 321 – 330.

Coxall, H., Wilson, P. A, Pälike, H., Lear, C. H., Backman, J., 2005. Rapid stepwise onset of Antarctic glaciation and deeper calcite compensation in the Pacific Ocean. Nature 433: 53 – 57.

Dale, B., 1983. 4. Dinoflagellate resting cysts: “benthic plankton”. In: Fryxell, G. A. (Editors), Survival strategies of the algae. Cambridge University Press, Cambridge and New York, pp. 69 – 136.

Dale, B., 1996. Chapter 31. Dinoflagellate cyst ecology: modelling and geological applications. In: Jansonius, J., McGregor, D. C. (Editors), Palynology: principles and applications, American Association of Stratigraphic Palynologists Foundation 3, pp. 1249 – 1275.

De Coninck, J. 1986. Organic walled phytoplankton from the Bartonian and Eo-Oligocene transitional deposits of the Woensdrecht Borehole, southern Netherlands. Mededelingen rijks geologische dienst 40-2: 1 – 49.

De Schepper, S., Head, M. J., Groeneveld, J., 2009. North Atlantic Current variability through marine isotope stage M2 (circa 3.3 Ma) during the mid-Pliocene. Paleoceanography 24: PA4206.

De Schepper, S, Fischer, E. I., Groeneveld, J., Head, M. J., Matthiessen, J., 2011. Deciphering the palaeoecology of Late Pliocene and Early Pleistocene dinoflagellate cysts. Palaeogeography, Palaeoclimatology, Palaeoecology 309: 17 – 32.

DeConto, R. M., Pollard, D., 2003. Rapid Cenozoic glaciation of Antarctica induced by declining atmospheric $CO_2$. Nature 421: 245 – 249.

Eldrett, J. S., Greenwood, D. R., Harding, I. C., Huber, M., 2009. Increased seasonality through the Eocene to Oligocene transition in northern high latitudes. Nature 459: 969 – 973.

Esper, O., Zonneveld, K. A. F., 2007. The potential of organic-walled dinoflagellate cysts for the reconstruction of past sea-surface conditions in the Southern Ocean. Marine Micropaleontology 65: 185 – 212.

Fensome, R. A., Taylor, F. J. R., Norris, G., Sarjeant, W. A. S., Wharton, D. I., 1993. A classification of living and fossil dinoflagellates. Micropaleontology Special papers, No. 7, 351 pp.

Fensome, R.A., Williams, G.L., 2004. The Lentin and Williams index of fossil dinoflagellates 2004 edition. American Association of Stratigraphic Palynologists Contributions Series 42: 1 – 909.

Frith, J V. 1996. 12 Upper Middle Eocene to Oligocene dinoflagellate biostratigraphy and assemblage variations in Hole 913B, Greenland Sea. Proceedings of the Ocean Drilling Program, Scientific Results 151: 203 – 242.

Gradstein, F. M., Ogg, J. G., Schmitz, M. D., Ogg, G. M. 2012. The Geologic Time Scale 2012. Elsevier, Oxford, UK.

Guerstein, G. R., Guler, M. V., Williams, G. L., Fensome, R. A., Chiesa, J. O., 2008. Middle Palaeogene dinoflagellate cysts from Tierra del Fuego, Argentina: biostratigraphy and palaeoenvironments. Journal of Micropalaeontology 27: 75 – 94.

Head, M. J., 1994. Morphology and paleoenvironmental significance of the Cenozoic dinoflagellate genera *Tectatodinium* and *Habibacysta*. Micropalaeontology 40: 289 – 321.

Head, M. J., Norris, G., 1989. Palynology and dinocyst stratigraphy of the Eocene and Oligocene in ODP Leg 105, Hole 647A, Labrador Sea. Proceedings of the Ocean Drilling Program, Scientific Results 105: 515 – 537.

Heilman-Clausen, C., Van Simaeys, S. 2005. Dinoflagellate cysts from the Middle Eocene to ?lowermost Oligocene succession in the Kysing Research Borehole, Central Danish Basin. Palynology 29: 143 – 204.

Houben, A. J. P., van Mourik, C. A., Montanari, A., Coccioni, R., Brinkhuis, H., 2012. The Eocene – Oligocene transition: Changes in sea level, temperature or both ? Palaeogeography, Palaeoclimatology, Palaeoecology 335 – 336: 75 – 83.

Jaramillo, C.A., Oboh-Ikuenobe, F. E., 1999. Sequence stratigraphic interpretations from palynofacies, dinocyst and lithological data of Upper Eocene-Lower Oligocene strata in southern Mississippi and Alabama, US Gulf Coast. Palaeogeography, Palaeoclimatology, Palaeoecology 145: 259 – 302.

Jeong, H. J., Yoo, Y. D., Kim, J. S., Seong, K. A., Kang, N. S., Kim, T. H., 2010. Ocean Science Journal 45: 65 – 91.

Jongman, R. H. G., ter Braak, C. J. F., Van Tongeren, O. F. R. 1995. Data analysis in community and landscape ecology. Cambridge University Press, Cambridge; New York, 324 pp.

771 Jovane, L., Coccioni, R., Marsili, A., Acton, G., 2009. The late Eocene greenhouse –
772 icehouse transition: Observations from the Massignano global stratotype section
773 and point (GSSP). In: Koeberl, C., Montanari, A. (Eds), The Late Eocene Earth –
774 Hothouse, Icehouse, and Impacts. Geological Society of America Special Paper
775 452: 149 – 168.
776
777 Köthe, A., 1990. Paleogene Dionoflagellates from Northwest Germany –
778 Biostratigraphy and Paleoenvironment. Geologisches Jahrbuch 118: 3 – 111.
779
780 Lear, C. H., Bailey, T. R., Pearson, P. N., Coxall. H. K., Rosenthal, Y., 2008. Cooling
781 and ice growth across the Eocene – Oligocene transition. Geology 36: 251 – 254.
782
783 Less, G., Özcan, E., 2012. Bartonian – Priabonian larger benthic foraminiferal events
784 in the Western Tethys. Austrian Journal of Earth Sciences 105: 129 – 140.
785
786 Liu, Z., Pagani, M, Zinniker, D., DeConto, R., Huber, M., Brinkhuis, H., Shah, S. R.,
787 Leckie, R. M., and Pearson, A., 2009. Global Cooling During the Eocene –
788 Oligocene Climate Transition. Science 323: 1187 – 1190.
789
790 MacLeod, N., Ortiz, N., Fefferman, N., Clyde, W., Schulter, C., MacLean, J., 2000. 5
791 – Phenotypic response of foraminifera to episodes of global environmental
792 change. In: Culver, S. J., Rawson, P. F. (Editors), Biotic Response to Global
793 Change, Cambridge University Press, Cambridge, pp. 51 – 78
794

MacRae, R.A., Fensome R.A., Williams, G.L., 1996. Fossil dinoflagellate diversity, originations and extinctions and their significance. Canadian Journal of Botany 74: 1687 – 1694.

Marret, F., Zonneveld, K. A. F., 2003. Atlas of modern organic-walled dinoflagellate cyst distribution. Review of Palaeobotany and Palynology 125: 1 – 200.

Masure, E., Vrielynck, B., 2009. Late Albian dinoflagellate cyst paleobiogeography as indicator of asymmetric sea surface temperature gradient on both hemispheres with southern high latitudes warmer than northern ones. Marine Micropaleontology 70: 120 – 133.

Matsuoka, K., Fukyo, Y., 2000. Technical Guide for Modern Dinoflagellate Cyst Study. WESTPAC-HAB/WESTPAC/IOC.

McMahon, J. M., 1997. Palynology and paleoecology of the Stone City Member, Crockett Formation, Middle Eocene, Burleston Co, Texas. Unpublished dissertation for degree of Master of Science. Texas A&M University, Texas, USA, 164 pp.

Mertens, K. N., Verhoeven, K., Verleye, T., Louwye, S., Amorim, A., Ribeiro, S., Deaf, A. S., Harding, I. C., De Schepper, S., González, C., Kodrans-Nsiah, M., De Vernal, A., Henry, M., Radi, T., Dybkjaer, K., Poulsen, N. E., Feist-Burkhardt, S., Chitolie, J., Heilmann-Clausen, C., Londeix, L., Turon, J.-L., Marret, F., Matthiessen, J., McCarthy, F. M. G., Prasad, V., Pospelova, V.,

Kyffin Hughes, J. E., Riding, J. B., Rochon, A., Sangiorgi, F., Welters, N., Sinclair, N., Thun, C., Soliman, A., Van Nieuwenhove, N., Vink, A., Young, M., 2009. Determining the absolute abundance of dinoflagellate cysts in recent marine sediments: The *Lycopodium* marker-grain method put to the test. Review of Palaeobotany and Palynology 157: 238 – 252.

Mudie, P. J., Harland, R., Matthiessen, J., De Vernal, A., 2001. Marine dinoflagellate cysts and high latitude Quaternary paleoenvironmental reconstructions: an introduction. Journal of Quaternary Science 16: 595 – 602.

Murray, S. A., Garby, T., Hoppenrath, M., Neilan, B. A., 2012. Genetic diversity, Morphological Uniformity and Polyketide Production in Dinoflagellates (*Amphidinium*, Dinoflagellata). PLoS ONE 7(6), e38253. doi:10. 1371/journal.pone.0038253.

Pagani, M., Huber, M., Liu, Z., Bohaty, S.M., Henderiks, J., Sijp, W., Krishnan, S., DeConto, R.M., 2011. The Role of Carbon Dioxide During the Onset of Antarctic Glaciation. Science 334: 1261 – 1264.

Pälike, H., Norris, R. D., Herrle, J. O., Wilson, P. A., Coxall, H. K., Lear, C. H., Shackleton, N. J., Tripati, A. K., Wade, B., 2006. The Heartbeat of the Oligocene Climate System. Science 314: 1894 – 1898.

Pearson, P. N., Foster, G. L., Wade, B. S., 2009. Atmospheric carbon dioxide through the Eocene – Oligocene climate transition. Nature 461: 1110 – 1113.

Peck, V. L., Yu, J., Kender, S., Riesselman, C. R., 2010. Shifting ocean carbonate chemistry during the Eocene – Oligocene climate transition: Implications for deep-ocean MG/Ca paleothermometry. Paleooceanography 25: PA4219.

Pound, M. J., Haywood, A. M., Salzmann, U., Riding, J. B., Lunt, D. J., Hunter, S. J. 2011. A Tortonian (late Miocene, 11.61 – 7.25 Ma) global vegetation reconstruction. Palaeogeography, Palaeoclimatology, Palaeoecology 300: 29 – 45.

Pound, M. J., Haywood, A. M., Salzmann, U., Riding, J. B., 2012. Global vegetational dynamics and latitudinal temperature gradients during the Mid to late Miocene (15.97 – 5.33 Ma). Earth Science Reviews 112: 1 – 22.

Salzmann, U., Haywood, A. M., Lunt, D. J., Valdes, P. J., Hill, D. J., 2008. A new global biome reconstruction and data model comparison for the Middle Pliocene. Global Ecology and Biogeography 17: 432 – 447.

Sarjeant, W. A., Lacalli, T., Gaines, G., 1987. The cysts and skeletal elements of dinoflagellates: speculations on the ecological causes for their morphology and development. Micropalaeontology 33: 1 – 36.

Schiøler, P., 2005. Dinoflagellate cysts and acritarchs from the Oligocene - Lower Miocene interval of the Alma-1X well, Danish North Sea. Journal of Micropalaeontology 24: 1 – 37.

Shipboard Scientific Party., 2001. Chapter 7, Site 1172. Proceedings of the Ocean Drilling Program, Initial Reports 189: 1 – 149 [CD-ROM].

Śliwińska, K. K., Clausen, O. R., Heilmann-Clausen, C., 2010. A mid-Oligocene cooling (Oi-2b) reflected in the dinoflagellate record and in depositional sequence architecture. An integrated study from the eastern North Sea Basin. Marine and Petroleum Geology 27: 1424 – 1430.

Sloan, L. C., Huber, M., 2001. Eocene Oceanic Responses to Orbital Forcing on Precessional Time Scales, Paleoceanography 16: 101 – 111.

Sluijs, A., Pross, J., Brinkhuis, H., 2005. From greenhouse to icehouse; organic-walled dinoflagellate cysts as palaeoenvironmental indicators in the Paleogene. Earth Science Reviews 68: 281 – 315.

Stern, R. F., Horak, A., Andrew, R. L., Coffroth, M.-A., Andersen, R. A., Küpper, F. C., Jameson, I., Hoppenrath, M., Véron, B., Kasai, F., Brand, J., James, E. R., Keeling, P. J., 2010. Environmental Barcoding Reveals Massive Dinoflagellate Diversity in Marine Environments. PLoS ONE 5(11), e13991, doi: 10.1371/journal.pone.0013991.

ter Braak, C. J. F., Smilauer, P. 1998. Canoco reference manual and user's guide to Canoco for Windows: software for canonical community ordination (version 4). Microcomputer Power, Ithaca, NY, 352 pp.

Vandenbroucke, T. R. A., Armstrong, H. A., Williams, M., Paris, F., Zalasiewicz, J. A., Sabbe, K., Nõlvak, J., Challands, T. J., Verniers, J., Servais, T. 2010. Polar front shift and atmospheric $CO_2$ during the glacial maximum of the Early Paleozoic Icehouse. PNAS 107: 14983 – 14986.

Van Mourik, C. A., Brinkhuis, H., Williams, G. L., 2001. Mid- to Late Eocene organic-walled dinoflagellate cysts from ODP Leg 171B, offhore Florida. Special Publication of the Geological Society, London 183: 225 – 251.

Van Simaeys, S. V., 2004. Stratigraphic and palaeoenvironmental analysis of the Rupelian and Chattian in their type regions: implications for global Oligocene chronostratigraphy. PhD Thesis, University of Leuven, 201 pp.

Van Simaeys, S., Musterman, D. K., Brinkhuis, H. 2005. Oligocene dinoflagellate cyst biostratigraphy of the southern North Sea Basin. Review of Palaeobotany and Palynology 134: 105 – 128.

Verleye, T. J., Louwye, S. 2010. Recent geographical distribution of organic-walled dinoflagellate cysts in the southeast Pacific (25 – 53°S) and their relation to the prevailing hydrographical conditions. Palaeogeography, Palaeoclimatology, Palaeoecology 298: 319 – 340.

Versteegh, G. J. M., Zonneveld, K. A. F., 1994. Determination of (palaeo-) ecological preferences of dinoflagellates by applying detrended and canonical

correspondence analysis to late Pliocene dinoflagellate cyst assemblages of the south Italian Singa section. Palynology 18: 264 – 265.

Wade, B. S., Kroon, D., 2002. Middle Eocene regional climate instability: Evidence from the western North Atlantic. Geology 30: 1011 – 1014.

Wade, B., Pälike, H., 2004. Oligocene climate dynamics. Paleoceanography 19: PA4019.

Wade, B. S., Pearson, P. N., 2008. Planktonic foraminiferal turnover, diversity fluctuations and geochemical signals across the Eocene/Oligocene boundary in Tanzania. Marine Micropalaeontology 68: 244 – 255.

Wade, B. S., Houben, A. J., Quaijtaal, W., Schouten, S., Rosenthal, Y., Miller, K. G., Katz, M. E., Wright, J. D., Brinkhuis, H. 2012. Multiproxy record of abrupt sea-surface cooling across the Eocene – Oligocene transition in the Gulf of Mexico. Geology 40: 159 – 162.

Wall, D., Dale, B., Lohmann, G. P., Smith, W. K., 1977. The environmental and climatic distribution of dinoflagellate cysts in Modern marine sediments from regions in the North and South Atlantic Oceans and adjacent seas. Marine Micropalaeontology 2: 121 – 200.

Wei, W., 1991. Evidence for an earliest Oligocene abrupt cooling in the surface waters of the Southern Ocean. Geology 19: 780 – 783.

Williams, G. L., Brinkhuis, H., Pearce, M. A., Fensome, R. A., Weegink, J. W., 2004. Southern Ocean and global dinoflagellate cysts events compared: index events for the Late Cretaceous – Neogene. In: Exon, N. F., Kennett, J. P., and Malone, M. J. (Eds.), Proceedings of the Ocean Drilling Program, Scientific Results 189: 1 – 98 [CD-ROM].

Yamazaki, A. K., Kamykowski, D., 2000. A dinoflagellate adaptive behavior model: response to internal biochemical cues. Ecological Modelling 134: 59 – 72.

Zonneveld, K. A., Marret, F., Versteegh, G. J. M., Bogus, K., Bonnet, S., Bouimetarhan, I., Crouch, E., de Vernal, A., Elshanawany, R., Edwards, L., Esper, O., Forke, S., Grøsfjeld, K., Henry, M., Holzwarth, U., Kielt, J.-F., Kim, S.-Y., Ladouceur, S., Ledu, D., Chen, L., Limoges, A., Londeix, L., Lu, S.-H., Mahmoud, M. S., Marino, G., Matsouka, K., Matthiessen, J., Mildenhal, D. C., Mudie, P., Neil., H. L., Pospelova, V., Qi, Y., Radi, T., Richerol, T., Rochon, A., Sangiorgi, F., Solignac, S., Turon, J.-L., Verleye, T., Wang, Y., Wang, Z., Young, M., 2013. Atlas of modern dinoflagellate cyst distribution based on 2405 datapoints. Review of Palaeobotany and Palynology 191: 1 – 197.

## Appendix 1A. Summary of locality data.

Longitude and latitude co-ordinates are decimalised. Where precise positions are uncertain, the co-ordinates are the origin of a specified geographical radius that the locality falls within. For full details see Supplementary Data.

### Mid Eocene (Bartonian)

| Locality Code | General Location | Modern Lat. | Modern Long. | Rotated Lat. | Rotated Long. | Locality Code | General Location | Modern Lat | Modern Long. | Rotated Lat. | Rotated Long. |
|---|---|---|---|---|---|---|---|---|---|---|---|
| B1 | UK | 50.72N | 1.75W | 48.55N | 5.64W | B37 | Southern Ocean | 46.78S | 144.96E | 67.23S | 149.59E |
| B2 | Siberia, Russia | 64.16N | 73.15E | 64.56N | 65.54E | B38 | North Sea | 59N | 1E | 56.87N | 3.49W |
| B3 | UK | 50.7N | 1.32W | 48.53N | 5.23W | B39 | North Sea | 57.76N | 1.95E | 55.65N | 2.51W |
| B4 | Germany | 53.05N | 11.45E | 51.17N | 6.85E | B40 | Slovakia | 49.22N | 19.35E | 43.89N | 16.97E |
| B5 | Germany | 52.38N | 9.96E | 50.46N | 5.47E | B41 | South Carolina, USA | 33.15N | 80.46W | 33.2N | 71.45W |
| B6 | North Atlantic | 29.98N | 76.52W | 29.74N | 67.86W | B42 | Antarctica | 61.85S | 42.93W | 61.74S | 51.57W |
| B7 | Siberia, Russia | 62.66N | 64.36E | 62.7N | 57.04E | B43 | Venezuela | 9.78N | 71.06W | 7.32N | 63.63W |
| B8 | Siberia, Russia | 61.76N | 63.6E | 61.77N | 56.46E | B44 | Venezuela | 9.32N | 70.68W | 6.87N | 63.24W |
| B9 | New Zealand | 41.53S | 173.58E | -53.73S | 176.39W | B45 | Venezuela | 9.38N | 70.55W | 6.94N | 63.11W |
| B10 | India | 23.25N | 72.5E | 8.79N | 66.03E | B46 | Venezuela | 9.2N | 70.78W | 6.75N | 63.33W |
| B11 | Antarctica | 64.28S | 56.75W | 64.09S | 59.81W | B47 | Georgia, USA | 32.93N | 81.65W | 33.08N | 72.66W |
| B12 | Antarctica | 64.22S | 56.63W | 64.03S | 59.69W | B48 | Georgia, USA | 33.03N | 81.7W | 33.18N | 72.69W |
| B13 | North Atlantic | 45N | 53W | 42.97N | 43.08W | B49 | Georgia, USA | 33.18N | 81.78W | 33.34N | 72.76W |
| B14 | Siberia, Russia | 66.76N | 77.46E | 67.33N | 69.26E | B50 | Georgia, USA | 33.23N | 81.9W | 33.39N | 72.87W |
| B15 | Siberia, Russia | 66.4N | 74.85E | 66.86N | 66.71E | B51 | Georgia, USA | 33.2 | 81.96 | 33.37 | 72.94 |
| B16 | Siberia, Russia | 67.46N | 75.96E | 67.96N | 67.54E | B52 | New Zealand | 45.66S | 170.65E | 53.13S | 167.83E |
| B17 | Japan | 34.45N | 134.85E | 42.11N | 129.39E | B53 | New Zealand | 45.28S | 170.85E | 52.77S | 167.52E |
| B18 | New Zealand | 45.28S | 170.83E | 52.77S | 167.54W | B54 | New Zealand | 45.9S | 170.43E | 53.35S | 168.14E |
| B19 | India | 22.83N | 88.43E | 4.34N | 80.1E | B55 | China | 39.5N | 75.98E | 39.12N | 70.15E |

| | | | | | | | | | | | |
|---|---|---|---|---|---|---|---|---|---|---|---|
| B20 | Argentina | 53.95S | 68.25W | 56.29S | 58.2W | B56 | Australia | 34.9S | 138.6E | 56.78S | 133.52E |
| B21 | North Atlantic | 67.65N | 56.68W | 65.38N | 41.45W | B57 | North Sea | 58.5N | 0.5W | 56.34N | 4.87W |
| B22 | North Atlantic, Greenland Sea | 75.48N | 6.95E | 70.53N | 13.07E | B58 | Kamchatka, Russia | 57.92 | 160.63 | 61.63 | 162.59 |
| B23 | France | 48.85N | 2.32E | 46.76N | 1.66W | B59 | Turkey | 41.65N | 33.68E | 38.63N | 41.42E |
| B24 | Netherlands | 51.45N | 4.3E | 49.4N | 0.11E | B60 | Novosibirsk, Russia | 54.58N | 77.02E | 55.18N | 71.05E |
| B25 | North Atlantic, Norwegian Sea | 67.7N | 1.03W | 63.95N | 4.78W | B61 | Kazakhstan | 51.98N | 76.15E | 52.55N | 70.48E |
| B26 | Denmark | 56.02N | 10.26E | 54.11N | 5.5E | B62 | Ukraine | 50.16N | 30E | 48.86N | 24.98E |
| B27 | India | 16.68N | 81.9E | 0.06S | 72.6E | B63 | India | 27.06N | 95.02E | 7.17N | 86.88E |
| B28 | Labrador Sea | 53.32N | 45.25W | 50.75N | 34.5W | B64 | Aral Sea | 47.16N | 61.13E | 47.11N | 55.9E |
| B29 | New Zealand | 42S | 173.75E | 54.08S | 175.82W | B65 | Italy | 39.93N | 16.46E | 34.79N | 13.37E |
| B30 | India | 25.33N | 90.68E | 6.31N | 82.68E | B66 | Hungary | 47.06N | 19.55E | 41.72N | 16.91E |
| B31 | France | 48.88N | 2.58E | 46.79N | 1.41W | B67 | Volgograd, Russia | 48N | 44.46E | 47.25N | 39.31E |
| B32 | France | 48.86N | 2.35E | 46.77N | 1.63W | B68 | Borneo | 3.25N | 110.72E | 7.31N | 113.7E |
| B33 | France | 48.83N | 2.48E | 46.74N | 1.5W | B69 | Spain | 41.48N | 1.38E | 39.7N | 1.85W |
| B34 | France | 48.93N | 2.45E | 46.84N | 1.54W | B70 | Slovakia | 48.66N | 19.65E | 43.31N | 17.17E |
| B35 | Argentina | 51.58S | 72.22W | 54.04S | 62.6W | B71 | Texas, USA | 30.63N | 96.55W | 31.92N | 87.86W |
| B36 | Southern Ocean | 45.03S | 144.32E | 65.71S | 147.17E | | | | | | |

972

973

## Early Oligocene (Rupelian)

| Locality | General | Modern | | Rotated | | Locality | General | Modern | | Rotated | |
|---|---|---|---|---|---|---|---|---|---|---|---|
| **Code** | **Location** | **Lat.** | **Long.** | **Lat.** | **Long.** | **Code** | **Location** | **Lat.** | **Long.** | **Lat.** | **Long.** |
| R1 | Belgium | 51.4N | 4.9E | 50.87N | 1.35E | R63 | Germany | 51.42N | 6.5E | 50.93N | 2.93E |
| R2 | Belgium | 51.2N | 5.1E | 50.67N | 1.56E | R64 | North Atlantic | 33.15N | 77.43W | 32.92N | 71.14W |
| R3 | Belgium | 51.1N | 5.36E | 50.58N | 1.82E | R65 | Egypt | 30.65N | 29.15E | 27.56N | 26.15E |
| R4 | Germany | 53.05N | 11.45E | 52.67N | 7.72E | R66 | North Atlantic | 53.32N | 45.25W | 51.82N | 38.03W |
| R5 | Germany | 52.53N | 7.3E | 52.05N | 3.65E | R67 | Turkey | 38.82N | 42.12E | 36.01N | 47.62E |
| R6 | Germany | 52.38 N | 9.96E | 51.97N | 6.29E | R68 | Turkey | 38.82N | 42.12E | 36.01N | 47.62E |
| R7 | Italy | 40.16N | 16.5E | 37.44N | 14.35E | R69 | Germany | 51.25N | 12.35E | 50.9N | 8.73E |
| R8 | Italy | 43.38N | 12.56E | 40.8N | 10.77E | R70 | Poland | 52.83N | 16.55E | 52.58N | 12.8E |

| | | | | | | | | | | | |
|---|---|---|---|---|---|---|---|---|---|---|---|
| R9 | Italy | 43.53N | 13.58E | 40.91N | 11.75E | R71 | Germany | 54N | 10.06E | 53.59N | 6.28E |
| R10 | Italy | 43.56N | 12.56E | 40.98N | 10.78E | R72 | Germany | 49.45N | 8.52E | 49N | 5.04E |
| R11 | Italy | 45.63N | 11.36E | 43.09N | 9.78E | R73 | Germany | 52.2N | 8.58E | 51.75N | 4.94E |
| R12 | Italy | 45.65N | 11.4E | 43.11N | 9.82E | R74 | Germany | 52.38N | 7.28E | 51.9N | 3.64E |
| R13 | Belgium | 51.25N | 4.38E | 50.71N | 0.84E | R75 | Germany | 52.52N | 13.42E | 52.19N | 9.71E |
| R14 | Poland | 49.33N | 20.93E | 46.45N | 19.14E | R76 | Turkey | 41.45N | 26.75E | 38.42N | 24.24E |
| R15 | North Sea | 55N | 6E | 54.49N | 2.2E | R77 | Nigeria | 5.35N | 6.5E | 3.05N | 2.9E |
| R16 | North Pacific | 52.56N | 161.2W | 45.17N | 143.71W | R78 | Belgium | 50.82N | 5.43E | 50.3N | 1.9E |
| R17 | Japan | 42.92N | 142.03E | 44.57N | 139.41E | R79 | Germany | 49.9N | 8.03E | 49.44N | 4.53E |
| R18 | Japan | 43.06N | 143.83E | 44.72N | 141.26E | R80 | France | 48.96N | 2.18E | 48.37N | -1.2W |
| R19 | Japan | 37N | 140.85E | 44.22N | 137.42E | R81 | France | 48.93N | 2.56E | 48.34N | 0.83W |
| R20 | North Atlantic | 45N | 53W | 43.78N | 46.22W | R82 | France | 48.95N | 2.92E | 48.37N | 0.47W |
| R21 | India | 22.83N | 88.43E | 9.42N | 83.94E | R83 | France | 48.8N | 2.12E | 48.2N | 1.25W |
| R22 | Australia | 34.33S | 142.4E | 51.08S | 138.85E | R84 | Barents Sea | 73.52N | 16.43E | 73.23N | 9.79E |
| R23 | Australia | 34.22S | 140.85E | 51.1S | 136.8E | R85 | Southern Ocean | 42.25S | 143.48E | 58.84S | 142E |
| R24 | North Atlantic | 63.35N | 7.78W | 62.53N | 12W | R86 | Southern Ocean | 43.92S | 154.28E | 58.97S | 157.63E |
| R25 | North Atlantic | 67.78N | 5.38E | 67.24N | 0.25E | R87 | Deleted due to poor age constraint | | | | |
| R26 | North Atlantic | 75.48N | 6.95E | 73.04N | 11.82E | R88 | Argentina | 53.83S | 67.7W | 55.5S | 58.19W |
| R27 | North Atlantic | 78.38N | 1.35E | 75.96N | 7.2E | R89 | Poland | 49.62N | 21.38E | 49.49N | 17.81E |
| R28 | South Atlantic | 51S | 46.96W | 51.67S | 37.32W | R90 | Mississippi, USA | 31.66N | 88.63W | 31.91N | 82.42W |
| R29 | South Atlantic | 47.56S | 24.63W | 47.08S | 15.43W | R91 | Alabama, USA | 31.58N | 88.1W | 31.81N | 81.89W |
| R30 | North Atlantic | 66.95N | 6.45W | 66.15N | 11.12W | R92 | Mississippi, USA | 31.72N | 88.66W | 31.97N | 82.44W |
| R31 | Tunisia | 36.26N | 8.9E | 33.83N | 6.78E | R93 | Mississippi, USA | 31.83N | 88.7W | 32.08N | 82.48W |
| R32 | Tunisia | 36.95N | 8.75E | 34.53N | 6.68E | R94 | North Sea | 57.76N | 1.95E | 57.15N | 2W |
| R33 | Southern Ocean | 43.95S | 149.92E | 59.7S | 151.64E | R95 | Antarctica | 77.18S | 163.7E | 77.66S | 155.45E |
| R34 | Southern Ocean | 42.6S | 144.4E | 59.09S | 143.4E | R96 | North Atlantic | 55.25N | 22.08W | 54.17N | 25.32W |
| R35 | France | 48.85N | 2.32E | 48.26N | 1.06W | R97 | North Atlantic | 67.78N | 5.38E | 67.24N | 0.25E |
| R36 | Italy | 43.53N | 13.58E | 40.91N | 11.75E | R98 | Florida, USA | 27.03N | 81.75W | 27N | 75.8W |
| R37 | Netherlands | 51.45N | 4.3E | 50.9N | 0.75E | R99 | Florida, USA | 27.36N | 81.43W | 27.31N | 75.46W |
| R38 | North | 67.7N | 1.03W | 67.02N | 5.98W | R100 | Florida, USA | 27.15N | 81.35W | 27.1N | 75.39W |

| | | | | | | | | | | | |
|---|---|---|---|---|---|---|---|---|---|---|---|
| | Atlantic | | | | | | | | | | |
| R39 | Denmark | 56.02N | 10.26E | 55.61N | 6.33E | R101 | Florida, USA | 27.7N | 80.43W | 27.61N | 74.44W |
| R40 | UK | 50.68N | 1.3W | 50.01N | 4.73W | R102 | Dunedin, New Zealand | 45.18S | 170.9E | 51.89S | 173.0W |
| R41 | India | 16.68N | 81.9E | 4.7N | 76.58E | R103 | Fiordland,New Zealand | 46.05S | 166.53E | 52.42S | 178.16W |
| R42 | Poland | 49.4N | 19.93E | 46.56N | 18.2E | R104 | Westland,New Zealand | 41.75S | 171.46E | 53.22S | 178.19E |
| R43 | Poland | 49.4N | 19.95E | 46.56N | 18.22E | R105 | China | 39.5N | 75.98E | 39.68N | 72.02E |
| R44 | Poland | 49.4N | 20.05E | 46.55N | 18.31E | R106 | Kazakhstan | 43.26N | 55.55E | 43.97N | 52.47E |
| R45 | Poland | 49.4N | 20.13E | 46.55N | 18.39E | R107 | Poland | 53.23N | 15.2E | 52.95N | 11.43E |
| R46 | Poland | 49.35N | 20.18E | 46.5N | 18.43E | R108 | Poland | 53.52N | 20.96E | 53.38N | 17.13E |
| R47 | Poland | 49.36N | 20.3E | 46.5N | 18.55E | R109 | Poland | 54.62N | 18.08E | 54.41N | 14.19E |
| R48 | Poland | 49.36N | 19.85E | 46.52N | 18.12E | R110 | Poland | 52.93N | 18.8E | 52.74N | 15.02E |
| R49 | Poland | 49.33N | 19.86E | 46.49N | 18.13E | R111 | Kamchatka, Russia | 57.92N | 160.63E | 60.07N | 163.41E |
| R50 | Poland | 49.33 | 19.96E | 46.48N | 18.22E | R112 | Albania | 41.33N | 19.82E | 38.5N | 17.6E |
| R51 | Poland | 49.33N | 19.93E | 46.49N | 18.2E | R113 | Rostov, Russia | 57.2N | 39.42E | 57.52N | 35.33E |
| R52 | Poland | 49.35N | 19.93E | 46.51N | 18.2E | R114 | Hungary | 47.06N | 19.55E | 44.23N | 17.68E |
| R53 | Poland | 49.38N | 20.13E | 46.53N | 18.39E | R115 | Volgograd, Russia | 48N | 44.46E | 48.45N | 41.04E |
| R54 | Poland | 49.3N | 19.86E | 46.46N | 18.13E | R116 | Slovakia | 48.66N | 19.65E | 45.83N | 17.88E |
| R55 | Poland | 49.28N | 19.83E | 46.44N | 18.1E | R117 | Romania | 47.22N | 23.18E | 44.28N | 21.14E |
| R56 | Poland | 49.28N | 19.95E | 46.44N | 18.21E | R118 | Ukraine | 48.63N | 23.88E | 45.67N | 21.88E |
| R57 | Poland | 49.28N | 19.86E | 46.44N | 18.13E | R119 | Romania | 46.28N | 26.58E | 46.29N | 23.18E |
| R58 | Poland | 49.28N | 19.95E | 46.44N | 18.21E | R120 | France | 46.08N | 6.48E | 45.59N | 3.2E |
| R59 | Poland | 49.3N | 19.92E | 46.46N | 18.18E | R121 | France | 46.05N | 6.38E | 45.56N | 3.1E |
| R60 | Poland | 49.36N | 19.82E | 46.52N | 18.09E | R122 | Egypt | 31.03N | 30.08E | 27.92N | 27.06E |
| R61 | Poland | 49.38N | 20.02E | 46.53N | 18.28E | R123 | Antarctica | 77S | 163.72E | 77.48S | 155.55E |
| R62 | South China Sea | 18.83N | 116.56E | 20.98N | 116.86E | R124 | Antarctica | 61.85S | 42.93W | 61.74S | 51.57W |

974

975

976

977

**Appendix 1B. Major categories of northern hemisphere latitudinal response, and constituent taxa, for dinoflagellate cysts occurring in both the Bartonian and Rupelian (see also: Supplementary Data: latitudinal ranges)**

W = low latitude / warm water form

C = high latitude / cold water form

M = mid-latitude/temperate form

H = heterotrophic

NB: taxa with broader ecological ranges, or for which different ecological assignments have previously been published, have not been classified below. For full details see Supplementary Data.

(i) Dinoflagellate species showing negligible change in their maximum northern hemisphere range between the Bartonian and Rupelian.

| | | | | | |
|---|---|---|---|---|---|
| *Achilleodinium biformoides* | *Deflandrea leptodermata* | H | W | *Phelodinium pumilum* | H |
| *Achilleodinium latispinosum* | *Deflandrea musculopsis* | H | | *Phthanoperidinium geminatum* | H |
| *Achomosphaera multifurcata* | *Deflandrea phosphoritica phosphoritica attenuata* | H | | *Phthanoperidinium levimurum* | H |
| *Achomosphaera triangulata* | *Deflandrea phosphoritica spinulosa* | H | | *Samlandia reticulifera* | |
| *Amphorosphaeridium multispinosum* | *Diphyes colligerum* | | | *Sentusidinium stipulatum* | |
| *Apteodinium maculatum* | *Distatodinium scariosum* | | | *Spiniferites microceras* | |
| *Areoligera undulata* | *Enneadocysta arcuata* | | | *Spiniferites ramosus granomembranaceus* | |
| *Areosphaeridium diktyoplokum* | *Florentinia laciniata* | | | *Spiniferites twistringiensis* | |

| | | | | | | | | | |
|---|---|---|---|---|---|---|---|---|---|
| | | | *propria* | | | | | | |
| *Batiacasphaera baculata* | | | *Gerdiocysta aciculata* | | | *Svalbardella cooksoniae* | H | C | |
| *Batiacasphaera micropapillata* | | | *Heteraulacacysta porosa* | | M | *Thalassiphora patula* | | | |
| *Bellatudinium hokkaidoanum* | | | *Homotryblium caliculum* | | | *Wetzeliella articulata* | H | | |
| *Cerebrocysta bartonensis* | | | *Homotryblium* | | | *Wetzeliella cf. clathrata* | H | | |
| | | | *tenuispinosum* | | | | | | |
| *Cerodinium leptodermum* | H | | *Impagidinium dispertitum* | | W | *Wetzeliella gochtii* | H | | |
| *Cerodinium wardense* | H | M | *Lejeunecysta hyalina* | H | | *Wetzeliella lunaris* | H | | |
| *Cyclonephelium compactum* | | | *Membranilarnacia* | | | *Wilsonidinium* | H | C | |
| | | | *angustivela* | | | *echinosuturatum* | | | |
| *Deflandrea granulata* | H | W | *Pentadinium taeniagerum* | | | | | | |

No. heterotrophic species = 18

(ii) Dinoflagellate species extending their maximum northern limit in the northern hemisphere in the Rupelian compared to the Bartonian

| | | | | | | | | | |
|---|---|---|---|---|---|---|---|---|---|
| *Achomosphaera crassipellis* | | | *Heteraulacacysta* | | | *Phthanoperidinium* | H | | |
| | | | *fehmarnensis* | | | *comatum* | | | |
| *Adnatosphaeridium robustum* | | | *Homotryblium floripes* | | | *Phthanoperidinium* | H | | |
| | | | | | | *coreoides* | | | |
| *Adnatosphaeridium vittatum* | | | *Homotryblium* | | | *Polysphaeridium asperum* | | | |
| | | | *oceanicum* | | | | | | |
| *Apectodinium homomorphum* | H | | *Homotryblium plectilum* | | | *Polysphaeridium subtile* | | | |
| *Apectodinium hyperacanthum* | H | | *Homotryblium vallum* | | | *Polysphaeridium zoharyi* | | W | |
| *Apteodinium australiense* | | | *Hystrichokolpoma* | | | *Polysphaeridium zoharyi* | | | |
| | | | *granulatum* | | | *subsp. ktana* | | | |
| *Apteodinium emslandense* | | | *Hystrichokolpoma* | | | *Rhombodinium perforatum* | H | M | |
| | | | *poculum* | | | | | | |
| *Caligodinium amiculum* | | | *Hystrichokolpoma* | | | *Riculacysta perforata* | | | |
| | | | *rigaudiae* | | | | | | |
| *Cleistosphaeridium ancyreum* | | | *Hystrichosphaeropsis* | | | *Selenopemphix armata* | H | | |
| | | | *rectangularis* | | | | | | |
| *Cleistosphaeridium* | | | *Hystrichostrogylon* | | | *Selenopemphix nephroides* | H | | |
| *diversispinosum* | | | *coninckii* | | | | | | |

| | | | | | | | | |
|---|---|---|---|---|---|---|---|---|
| *Cleistosphaeridium placacanthum* | | | *Hystrichostrogylon membraniphorum* | | | *Selenpemphix selenoides* | H | |
| *Cordosphaeridium cantharellus* | | | *Impagidinium maculatum* | | W | *Spiniferella cornuta* | | |
| *Cordosphaeridium minimum* | | | *Impagidinium paradoxum* | | | *Spiniferites bulloideus* | | |
| *Cordosphaeridium robustum* | | | *Impletosphaeridium kroemmelbeinii* | | | *Spiniferites hyperacanthus* | | |
| *Dapsilidinium pastielsi* | | | *Impletosphaeridium ligospinosum* | | | *Spiniferites membranaceus* | | |
| *Deflandrea heterophlycta* | H | | *Impletosphaeridium multispinosum* | | | *Spiniferites mirabilis* | | W |
| *Deflandrea oebisfeldensis* | H | M | *Impletosphaeridium rugosum* | | | *Spiniferites perforatus* | | |
| *Deflandrea phosphoritica* | H | | *Lejeunecysta cinctoria* | H | | *Spiniferites pseudofurcatus* | | |
| *Deflandrea phosphoritica australis* | H | | *Lejeunecysta fallax* | H | | *Spiniferites ramosus* | | |
| *Dinopterygium cladoides* | | M | *Lejeunecysta tenella* | H | | *Spiniferites ramosus gracilis* | | |
| *Diphyes ficusoides* | | M | *Lingulodinium machaerophorum* | | W | *Surculosphaeridium? oceaniae* | | |
| *Distatodinium paradoxum* | | | *Lingulodinium pycnospinosum* | | | *Tectatodinium pellitum* | | W |
| *Distatodinium tenerum* | | | *Litosphaeridinium mamellatum* | | | *Thalassiphora pelagica* | | |
| *Dracodinium laszczynskii* | H | | *Melitasphaeridium asterium* | | | *Thalassiphora reticulata* | | |
| *Elytrocysta brevis* | | | *Membranophoridium aspinatum* | | | *Thalassiphora velata* | | W |
| *Fibrocysta vectensis* | | | *Nematosphaeropsis reticulensis* | | | *Trinovantedinium boreale* | | |
| *Glaphyrocysta intricata* | | | *Operculodinium centrocarpum* | | W | *Tubiosphaera magnifica* | | |
| *Glaphyrocysta microfenestrata* | | | *Operculodinium eisenackii* | | | *Turbiosphaera symmetrica* | | |
| *Glaphyrocysta pastielsi* | | | *Operculodinium tiara* | | | *Wetzeliella ovalis* | H | |
| *Glaphyrocysta paupercula* | | | *Operculodinium* | | | *Wetzeliella simplex* | H | |

| | | | |
|---|---|---|---|
| | *uncinispinosum* | | |
| *Glaphyrocysta reticulosa* | *Operculodinium xanthium* | | cf. *Wetzeliella symmetrica* |
| *Glaphyrocysta vicina* | *Palaeocystodinium golzowense* | H | *Xenicodinium conispinum* |
| *Glyphanodinium facetum* | *Pentadinium laticinctum granulatum* | | *Ynezidinium brevisulcatum* |
| *Gonyaulacysta giuseppei* | *Pentadinium lophophorum* | | |
| *Heteraulacacysta campanula* | *Phthanoperidinium eocenicum* | H | |

No. heterotrophic species = 20

(iii) Dinoflagellate species with a reduced maximum northern limit in the northern hemisphere in the Rupelian compared to the Bartonian

| | | | |
|---|---|---|---|
| *Achomosphaera alcicornu* | *Eocladopyxis peniculata* | *Pentadinium goniferum* | |
| *Achomosphaera ramulifera* | *Fibrocysta axialis* | *Pentadinium laticinctum* | |
| *Adnatosphaeridium multispinosum* | *Glaphyrocysta divaricata* | *Phthanoperidinium alectrolophum* | H |
| *Areoligera coronata* | *Glaphyrocysta exuberans* | *Phthanoperidinium filigranum* | H |
| *Areoligera senonensis* | *Glaphyrocysta laciniiformis* | *Phthanoperidinium multispinum* | H |
| *Areoligera sentosa* | *Glaphyrocysta ordinata* | *Phthanoperidinium resistente* | H |
| *Areoligera tauloma* | *Glaphyrocysta semitecta* | *Phthanoperidinium stockmansii* | H |
| *Areosphaeridium michoudii* | *Glaphyrocysta texta* | *Polysphaeridium congregatum* | |
| *Batiacasphaera compta* | *Heteraulacacysta leptalae* | *Pterodinium cingulatum* | |
| *Batiacasphaera hirsuta* | *Homotryblium abbreviatum* | *Pyxidiella scrobiculata* | H |

| | | | | | | | |
|---|---|---|---|---|---|---|---|
| *Charlesdownia reticulata* | H | | *Homotryblium pallidum* | | | *Rhombodinium draco* | H | M |
| *Charlesdownia variabilis* | H | | *Homotryblium floripes brevіradiatum* | | | *Rhombodinium longimanum* | H | |
| *Cordosphaeridium exilimurum* | | | *Hystrichokolpoma cinctum* | | M | *Rhombodinium porosum* | H | |
| *Cordosphaeridium fibrospinosum* | | | *Hystrichokolpoma globulus* | | W | *Rottnestia borussica* | | C |
| *Cordosphaeridium funiculatum* | | | *Hystrichokolpoma salacia* | | | *Samlandia chlamydophora* | | |
| *Cordosphaeridium gracile* | | | *Hystrichosphaeridium tubiferum* | | M | *Selenopemphix coronata* | H | |
| *Cordosphaeridium inodes* | | | *Impagidinium aculeatum* | | W | *Spiniferites cornuta* | | |
| *Corrudinium incompositum* | | | *Impagidinium velorum* | | | *Spiniferites monilis* | | |
| *Cribroperidinium giuseppei* | | | *Impletosphaeridium insolitum* | | | *Spiniferites ramosus granosus* | | |
| *Dapsilidinium pseudocolligerum* | | | *Lentinia serrata* | H | | *Sumatradinium hispidum* | H | |
| *Dapsilidinium simplex* | | | *Lentinia? wetzelii* | H | | *Tanyosphaeridium regulare* | | |
| *Deflandrea arcuata* | H | W | *Melitasphaeridium pseudorecurvatum* | | | *Thalassiphora delicata* | | |
| *Deflandrea denticulata* | H | | *Microdinium reticulatum* | | | *Thalassiphora fenestrata* | | |
| *Distatodinium craterum* | | | *Nematosphaeropsis lemniscata* | | | *Turbiosphaera galatea* | | |
| *Distatodinium ellipticum* | | | *Operculodinium divergens* | | | *Wilsonidium intermedium* | H | |
| *Enneadocysta multicornuta* | | | *Operculodinium microtriainum* | | | *Wilsonidium tabulatum* | H | |
| *Enneadocysta pectiniformis* | | M | *Paucisphaeridium inversibuccinum* | | | | | |

No. heterotrophic species = 19

**Figure and Table captions**

Fig. 1. Eocene – Oligocene geochronology and temporal $\delta^{18}O$ curve showing key climate events. Based on Gradstein et al. (2012, fig. 28.11). NB: Wade et al (2012) show the Eocene – Oligocene boundary at about 33.7 Ma

Fig. 2. Bartonian stratigraphy and age ranges of successions investigated as part of this study. Range bars do not necessarily imply the presence of all the corresponding stratigraphical units. Ages and correlations of stratigraphical units based on Gradstein et al. (2012). Locality details are summarised in Appendix 1A. For source literature and comprehensive data relating to these localities, see Supplementary Data.

Fig. 3. Rupelian stratigraphy and age ranges of successions investigated as part of this study. Range bars do not necessarily imply the presence of all the corresponding stratigraphical units. Ages and correlations of stratigraphical units based on Gradstein et al. (2012). Locality details are summarised in Appendix 1A. For source literature and comprehensive data relating to these localities, see Supplementary Data.

Fig. 4. Global data and palaeogeography maps. (A, B): maps showing the modern and Bartonian/Rupelian palaeo co-ordinates of data points used in this study. See Supplementary Data for individual locality details; (C, D): Eocene and Oligocene palaeogeography based on maps produced by Ron Blakey, Colorado Plateau Geosystems.

Fig. 5. DCA sample scatter plots of the (A) Bartonian (460 species, 71 samples) and (B) Rupelian (486 species, 122 samples) datasets (note that outlier sample R41 was omitted). Northern Hemisphere samples = filled symbols, Southern Hemisphere samples = open symbols

Fig. 6. DCA sample scatter plots of the Bartonian (A, B - 365 species, 55 samples) and Rupelian (C, D – 449 species, 106 samples) Northern Hemisphere datasets. (A, C): symbols represent ocean basins. Arctic Ocean: black squares; Atlantic Ocean: dark grey circles; Tethys Ocean: brown diamonds; North Sea: pink diamonds; Indian Ocean: beige stars; Pacific Ocean: light grey squares. (B, D): colours represent northern latitude classes. 80 – 70°: darkest blue-purple; 70 – 60°: dark blue; 60 – 50°: light blue; 50 – 40°: green; 40 – 30°: yellow; 30 – 20°: orange; 10 – 0°: red.

Fig. 7. DCA sample scatter plot of combined Bartonian-Rupelian dataset (only offshore Atlantic and Arctic locations, see text for more details) with 15 active Bartonian samples (filled symbols) and 21 supplementary Rupelian samples (open symbols). For colour coding of latitude classes, see legend Fig. 6 B, D.

Fig. 8. Geographical plots for selected species showing change in global occurrence between the Bartonian and Rupelian. Species are plotted using palaeo co-ordinates on a modern base map.

Fig. 9. Global plots of temperature sensitive / latitudinally diagnostic dinoflagellate cyst taxa that occur in both the Bartonian and Rupelian. (A): Bartonian global

distribution of warm-water/ low-latitude indicator dinoflagellate cyst taxa; (B): Rupelian global distribution of warm-water / low-latitude indicator dinoflagellate cyst taxa; (C): Bartonian global distribution of cool-water / high-latitude indicator dinoflagellate cyst taxa; (D) Rupelian global distribution of cold-water / high-latitude indicator dinoflagellate cyst taxa.

Table 1. The temperature/latitude affinities of dinoflagellate cyst taxa occurring in both the Bartonian and Rupelian, based on published literature. Excludes species interpreted as broad-ranging / mid-latitude / temperate or cosmopolitan, except for instances where this is contradicted by multiple literature records. Latitude assignments are qualified NH (Northern Hemisphere) or SH (southern hemisphere), where it is not known from the source literature if this can be extrapolated to both hemispheres.

Supplementary Fig. 1. DCA sample scatter plots, Northern Hemisphere datasets, showing North Sea, Atlantic Ocean and Arctic Ocean samples only. Bartonian: 39 samples (318 species), outliers (20, 35) removed; Rupelian: 49 samples (356 species), outliers (77, 28, 29, 88) removed. Symbols represent ocean basins: Arctic Ocean = black squares; Atlantic Ocean = dark grey circles; North Sea = pink diamonds. Fill of symbols distinguishes inshore (open) and offshore (filled). Also see TextFig. 6 (A, C).

Supplementary Fig. 2. DCA sample scatter plots, Northern Hemisphere datasets, showing North Sea and Atlantic Ocean samples only. Bartonian : 31 samples (282 species), outliers (20, 35) removed; Rupelian: 48 samples (350 species), outliers (77, 28, 29, 88) removed. Symbols represent ocean basins: Atlantic Ocean = dark grey

circles; North Sea = pink diamonds. Fill of symbols distinguishes inshore (open) and offshore (filled). Also see TextFig. 6 (A, C).

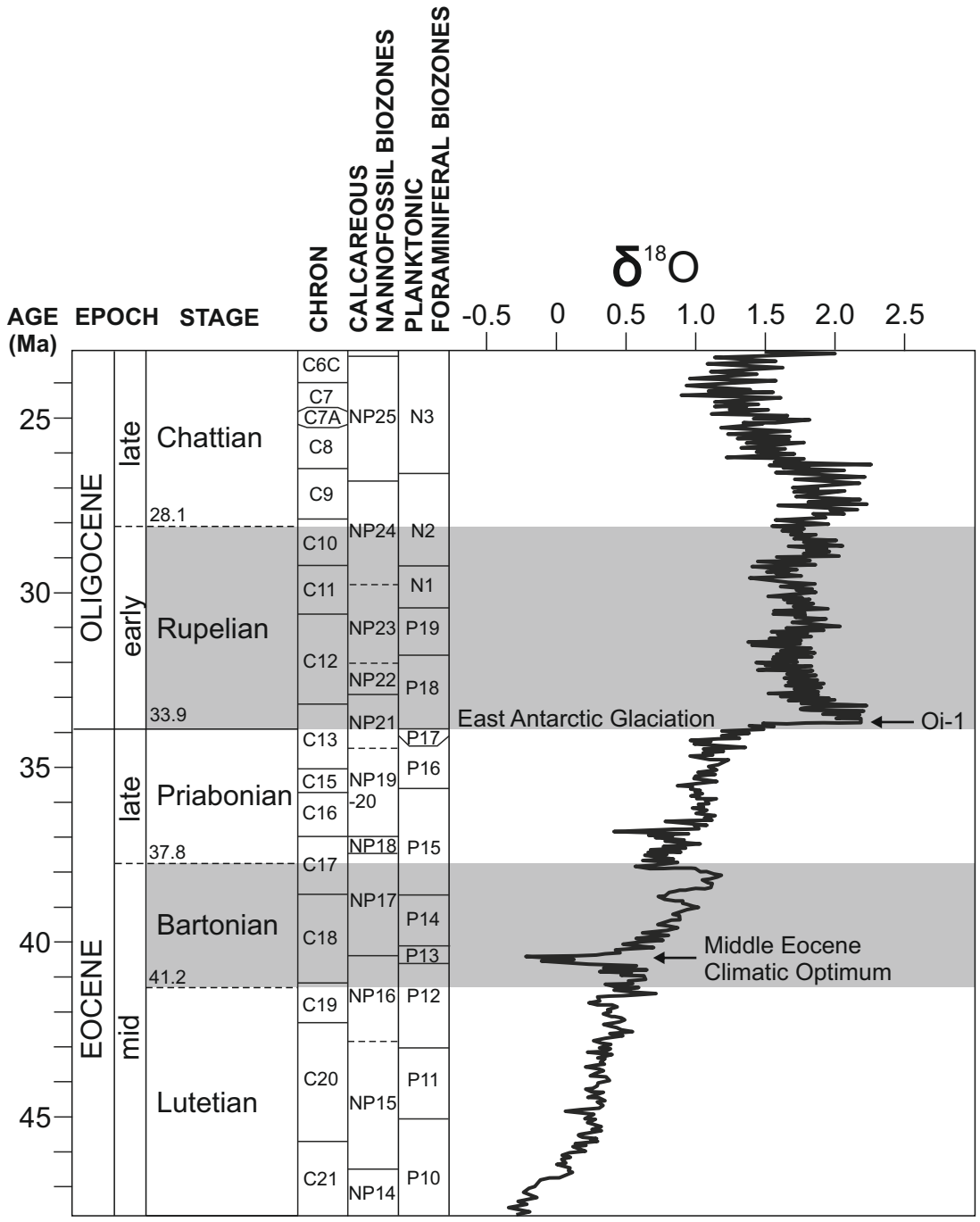
AGE (Ma)
EPOCH
STAGE
CHRON
CALCAREOUS NANNOFOSSIL BIOZONES
PLANKTONIC FORAMINIFERAL BIOZONES
δ18O
-0.5
0
0.5
1.0
1.5
2.0
2.5
25
30
35
40
45
OLIGOCENE
EOCENE
late
early
mid
late
Chattian
28.1
Rupelian
33.9
Priabonian
37.8
Bartonian
41.2
Lutetian
C6C
C7
C7A
C8
C9
C10
C11
C12
C13
C15
C16
C17
C18
C19
C20
C21
NP25
NP24
NP23
NP22
NP21
NP19-20
NP18
NP17
NP16
NP15
NP14
N3
N2
N1
P19
P18
P17
P16
P15
P14
P13
P12
P11
P10
East Antarctic Glaciation
Oi-1
Middle Eocene Climatic Optimum

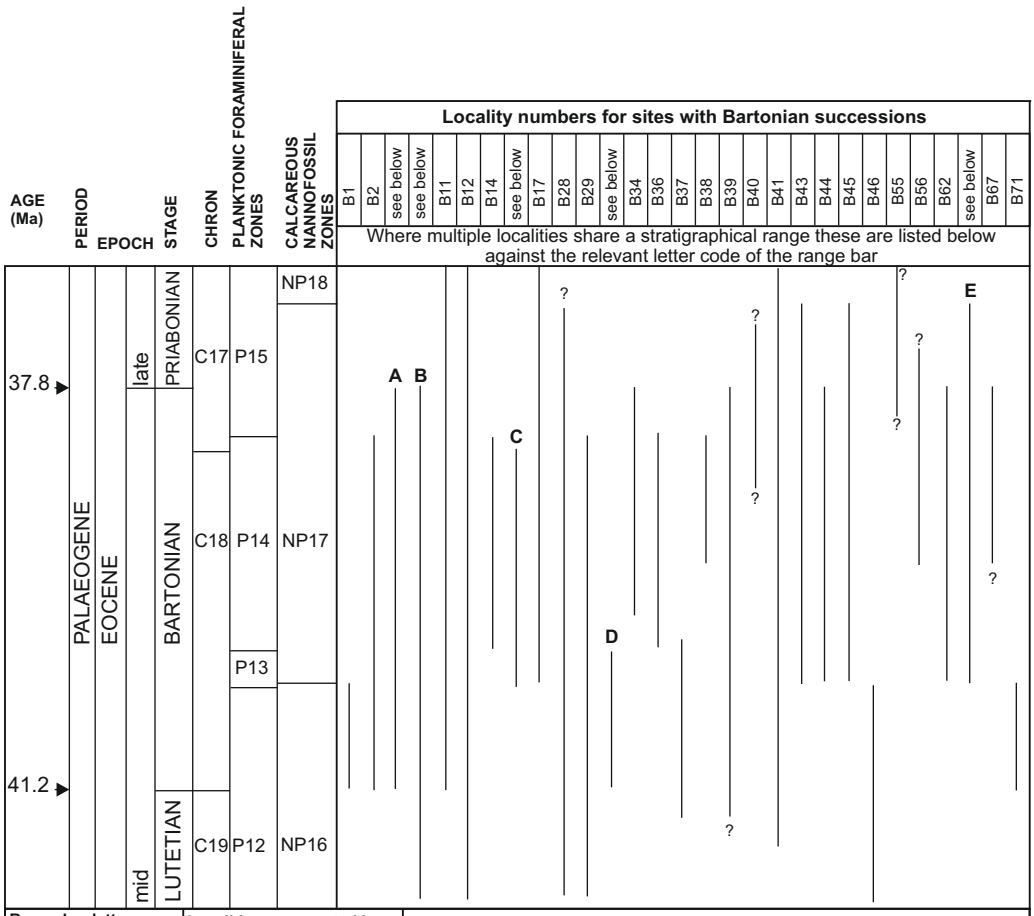


| Range bar letter shown in above figure | Localities represented by range bar |
|---|---|
| A | B3-6; 8; 10; 21-27; 31; 57-58; 60-61; 63-64; 68-69 |
| B | B7; 9, 13, 18-20; 30; 35; 42; 47-54; 59 |
| C | B15-16 |
| D | B32-33 |
| E | B65-66; 70 |

**Supplementary age information**

B11: probably includes Priabonian
B12, B20: could include Lutetian & Priabonian
B13, B42: could include Lutetian
B17: youngest age may include NP20 (Priabonian)
B19, B30: Bartonian and/or Lutetian
B35: includes Lutetian and ?Ypresian
B47-54: includes mid Lutetian

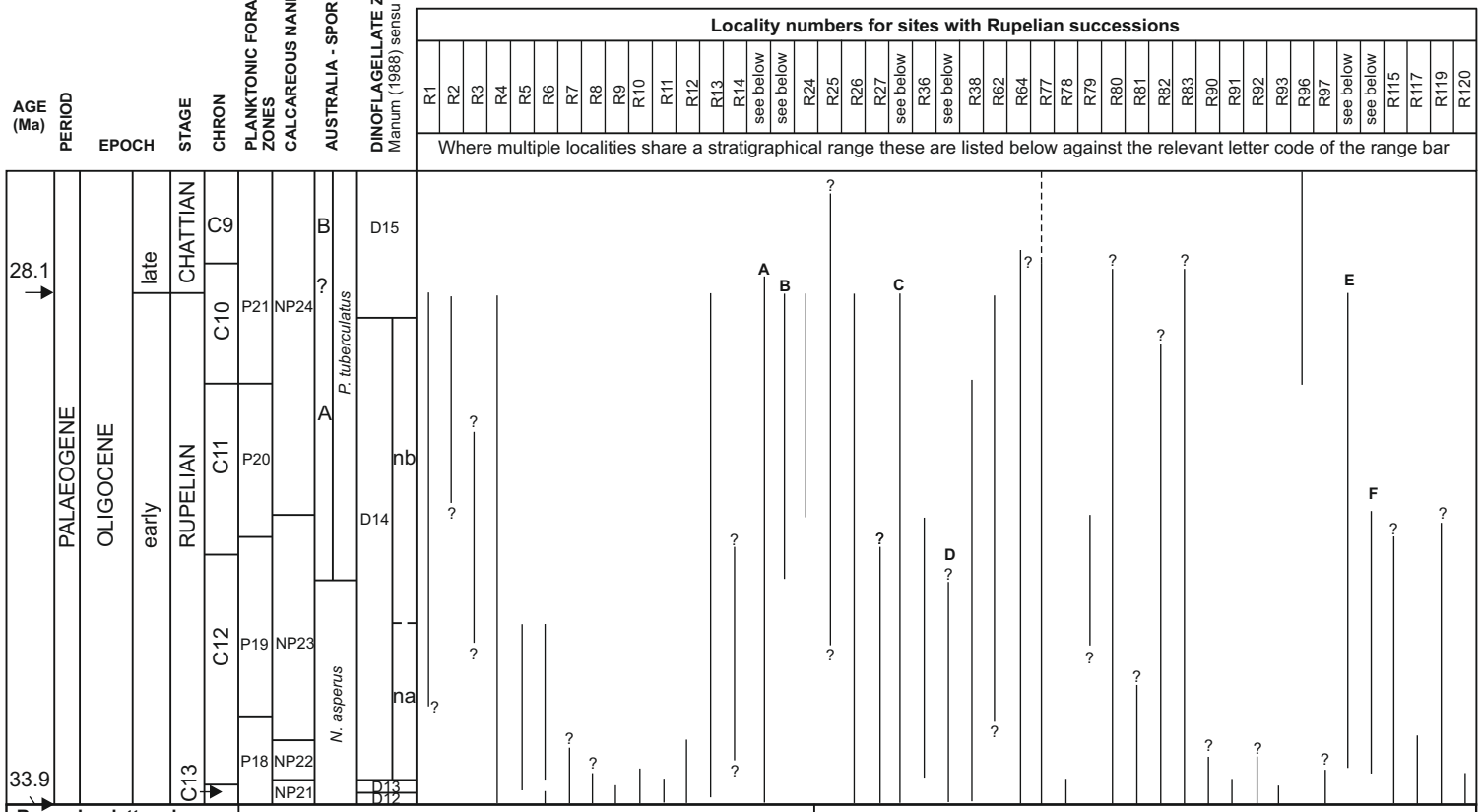


| Range bar letter shown in above figure | Localities represented by range bar | Supplementary age information |
|---|---|---|
| A | R 15-21 | R38: probably excludes youngest Rupelian<br>R77: may include Chattian<br>R86: may include latest Eocene and Chattian<br>R88: includes latest part of Late Eocene (Priabonian)<br>R96: includes NP25 (Chattian)<br>R102, R104: includes late Priabonian<br>R103: includes Late Eocene<br>R123: probably includes latest Eocene<br>R87: deleted from this study because of uncertainty about its age relationship |
| B | R 22-23 | |
| C | R 28-35; 39; 41-61; 63; 65-76;84-86; 88-89; 94-95; 98-106; 108-109; 111-113; 118; 121-124 | |
| D | R 37, 40 | |
| E | R 107, 110 | |
| F | R 114, 116 | |

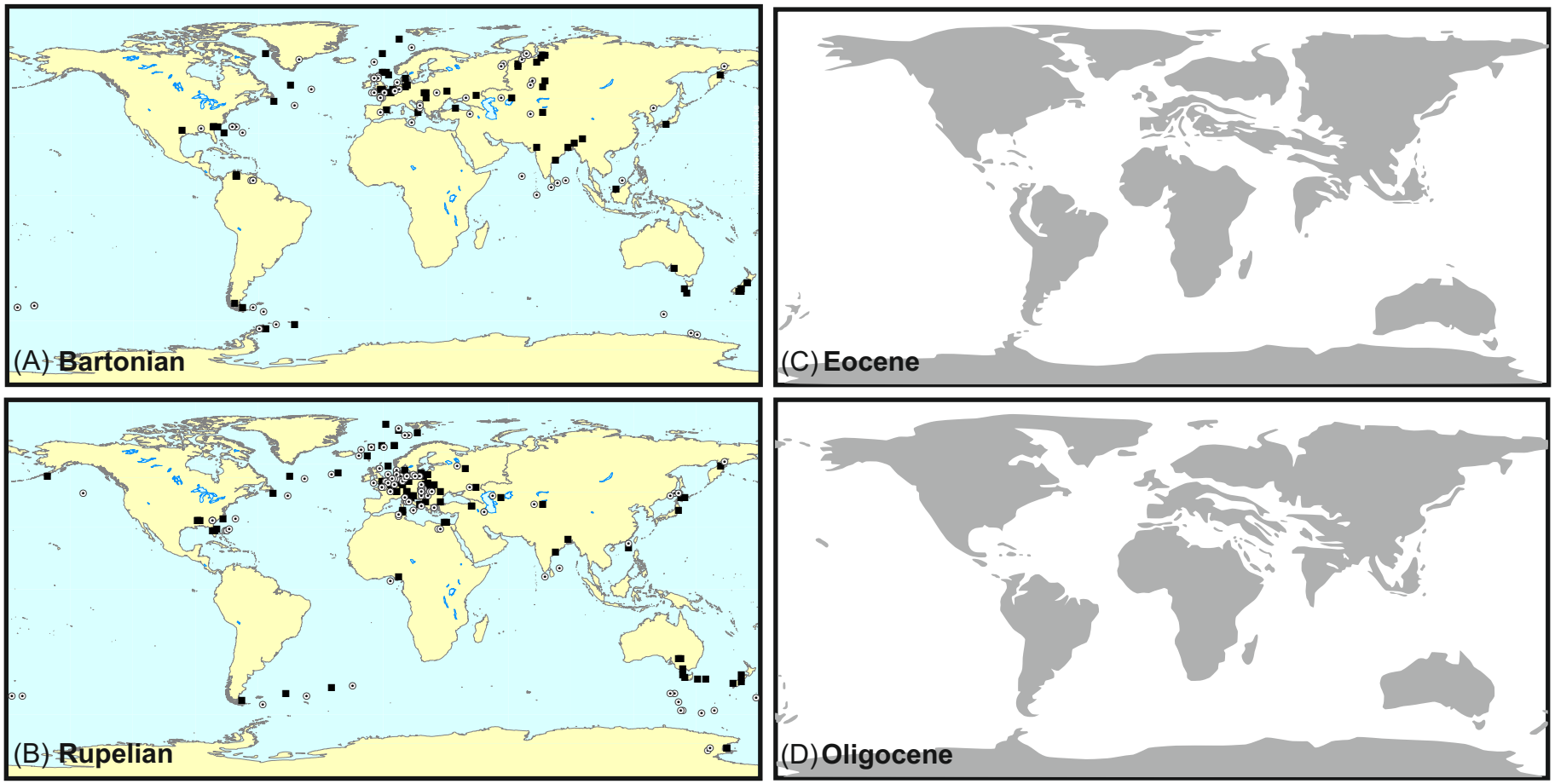


■ data point; modern co-ordinates

⊙ data point; palaeo co-ordinates

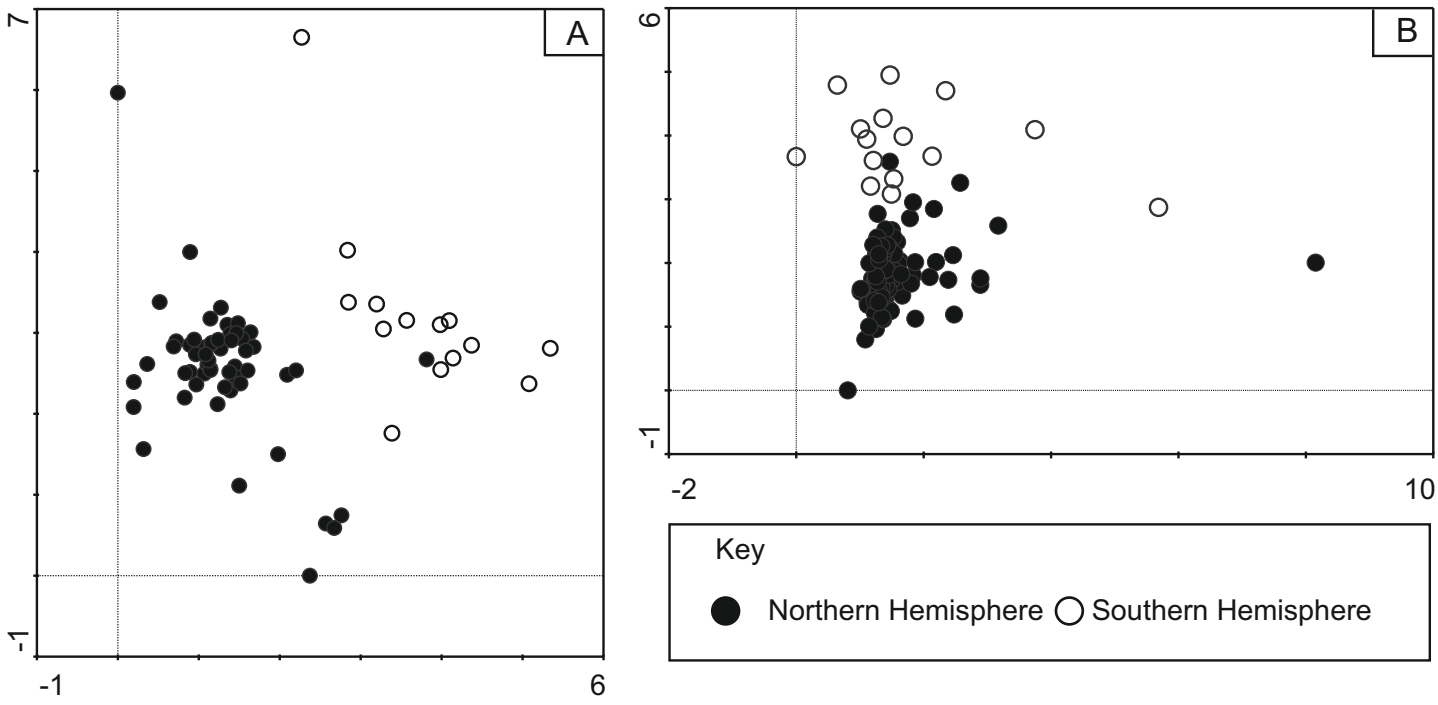
A
7
-1
-1
6
B
6
-1
-2
10
Key
Northern Hemisphere
Southern Hemisphere

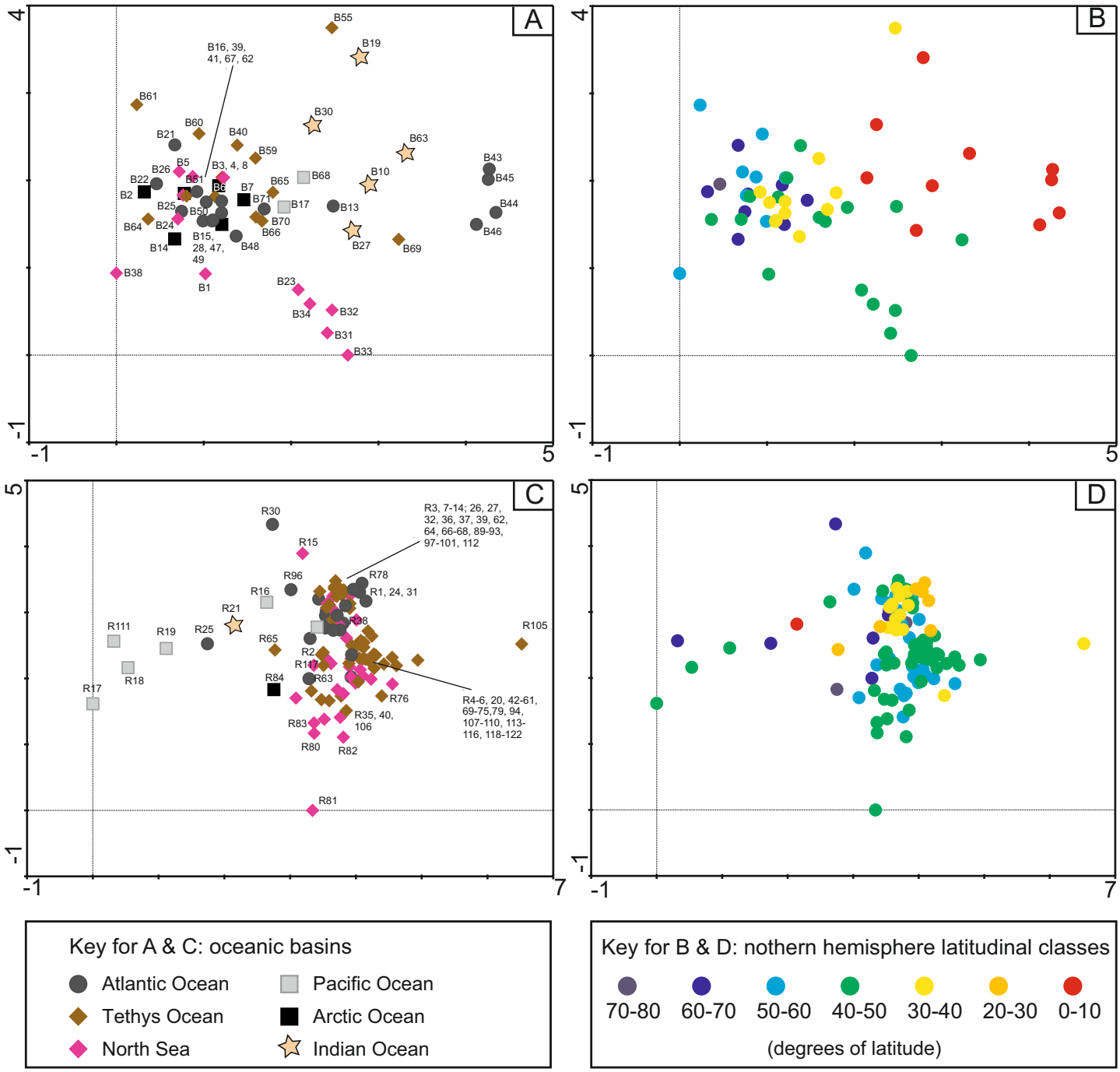


Key for A & C: oceanic basins

- Atlantic Ocean
- Pacific Ocean
- Tethys Ocean
- Arctic Ocean
- North Sea
- Indian Ocean

Key for B & D: nothern hemisphere latitudinal classes

70-80 | 60-70 | 50-60 | 40-50 | 30-40 | 20-30 | 0-10

(degrees of latitude)

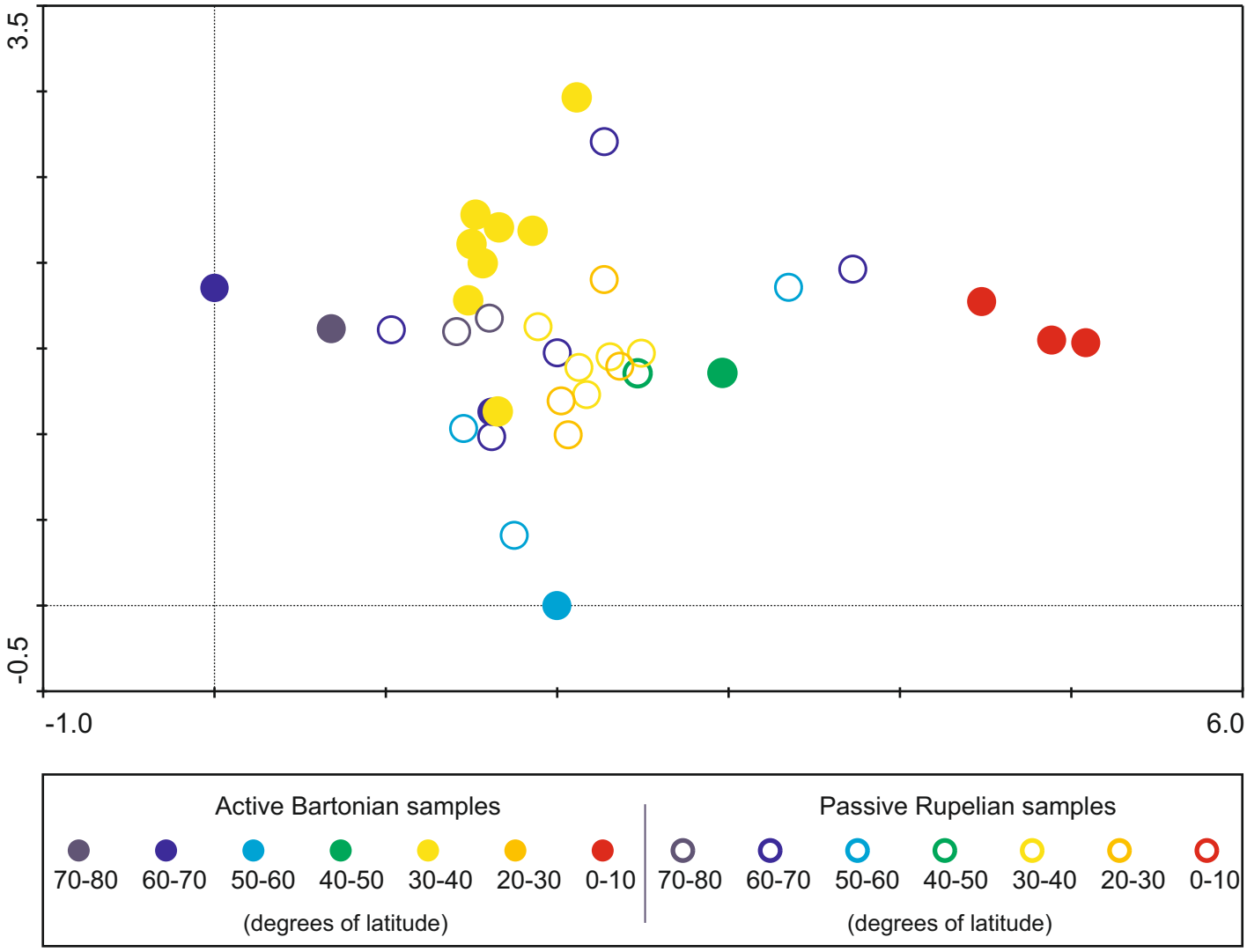
3.5
-0.5
-1.0
6.0
Active Bartonian samples
70-80
60-70
50-60
40-50
30-40
20-30
0-10
(degrees of latitude)
Passive Rupelian samples
70-80
60-70
50-60
40-50
30-40
20-30
0-10
(degrees of latitude)

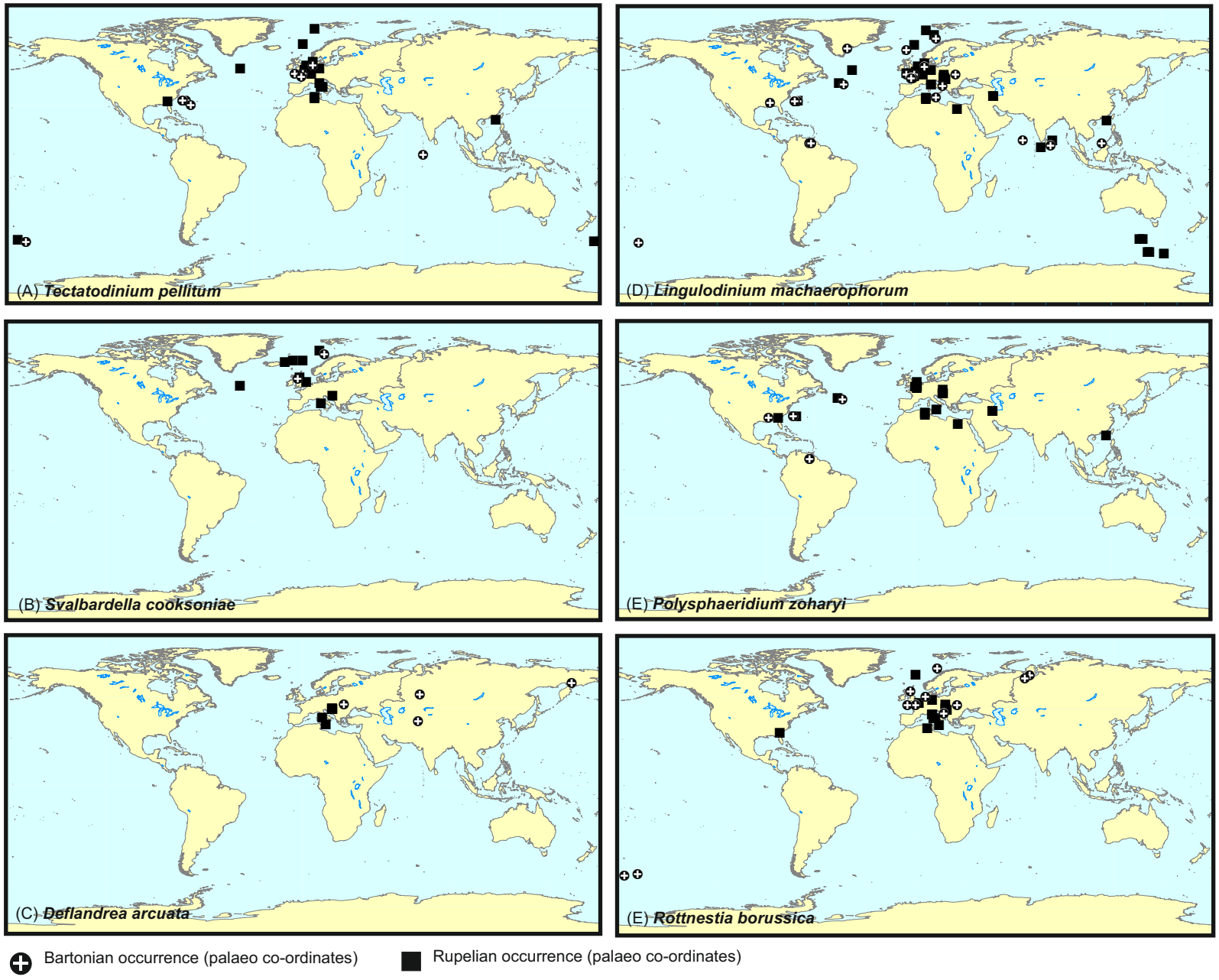
(A) Tectatodinium pellitum
(D) Lingulodinium machaerophorum
(B) Svalbardella cooksoniae
(E) Polysphaeridium zoharyi
(C) Deflandrea arcuata
(E) Rottnestia borussica
Bartonian occurrence (palaeo co-ordinates)
Rupelian occurrence (palaeo co-ordinates)

| | TAXON | INTREPRETATION | REFERENCE |
|---|---|---|---|
| Temperature / latitude diagnostic species that have not been variably interpreted by different authors | *Deflandrea antarctica* | High latitude(SH) | Williams et al. (2004) |
| | *Deflandrea arcuata* | Low latitude (exclusively) | Brinkhuis & Biffi (1993) |
| | *Deflandrea leptodermata* | Low latitude (exclusively) | Brinkhuis & Biffi (1993) |
| | *Hystrichokolpoma globulus* | Low latitude (exclusively) | Brinkhuis & Biffi (1993) |
| | *Hystrichosphaeridium truswelliae* | High latitude (SH) | Williams et al. (2004) |
| | *Impagidinium dispertitum* | Low latitude (exclusively) | Brinkhuis & Biffi (1993) |
| | *Impagidinium maculatum* | Low latitude (exclusively) | Brinkhuis & Biffi (1993) |
| | *Lingulodinium machaerophorum* | Warm water | Marret & Zonneveld (2003) |
| | *Octodinium askiniae* | High latitude (SH) | Williams et al. (2004) |
| | *Operculodinium israelianum* | Tropical - temperate water | Marret & Zonneveld (2003);<br>De Schepper et al. (2009) |
| | *Polysphaeridium zoharyi* | Warm water | Head & Norris (1989);<br>Marret & Zonneveld (2003) |
| | *Rottnestia borussica* | High latitude | Brinkhuis & Biffi (1993) cited in<br>Van Mourik et al. (2001) |
| | *Spinidinium macmurdoense* | High latitude (SH) | Williams et al. (2004) |
| | *Spiniferites mirabilis* | Warm water | McMahon (1997);<br>Marret & Zonneveld (2003);<br>De Schepper et al. (2009) |
| | *Svalbardella cooksoniae* | Cold water | Van Simaeys (2004) |
| | *Tectatodinium pellitum* | Warm water | Head (1994) cited in Jaramillo et al. (1999);<br>Marret & Zonneveld (2003) |
| | *Thalassiphora velata* | Low latitude (exclusively) | Brinkhuis & Biffi (1993) |
| | *Wilsonidinium echinosuturatum* | High latitude (SH) | Williams et al. (2004) |
| Temperature / latitude diagnostic species that have been variably interpreted by different authors | *Achomosphaera alcicornu* | Low to high latitudes<br>High latitude | Williams et al. (2004)<br>Brinkhuis & Biffi (1993), cited in<br>Van Mourik et al. (2001) |
| | *Corrudinium incompositum* | Mid latitude, low latitude<br>High latitude | Williams et al. (2004)<br>Brinkhuis & Biffi (1993) cited in<br>Van Mourik et al. (2001) |
| | *Deflandrea granulata* | Low latitude (exclusively)<br>Transantarctic Flora | Brinkhuis & Biffi (1993)<br>Guerstein et al. (2008) |
| | *Glaphyrocysta semitecta* | Mid latitude (NH), low latitude<br>High latitude | Williams et al. (2004)<br>Brinkhuis & Biffi (1993) cited in<br>Van Mourik et al. (2001) |
| | *Hystrichosphaeridium tubiferum* | Mid latitude (NH)<br>Transantarctic Flora | Williams et al. (2004)<br>Guerstein et al. (2008) |
| | *Operculodinium centrocarpum* | Warm-temperate<br>Cosmopolitan (Arctic to tropical) | McMahon (1997)<br>De Schepper et al. (2009) |
| | *Schematophora speciosa* | Low latitude, mid latitude (SH), high latitude (SH)<br>Warm water<br>Low latitude (exclusively) | Williams et al. (2004)<br>Shipboard Scientific Party (2001)<br>Brinkhuis & Biffi (1993) |
| | *Selenopemphix nephroides* | Cold water<br>Extremely warm water | Guerstein et al. (2008)<br>Marret & Zonneveld (2003) |
| | *Stoveracysta ornata* | Low latitude, mid latitude (SH), high latitude (SH)<br>Low latitude (exclusively) | Williams et al. (2004)<br>Brinkhuis & Biffi (1993) |

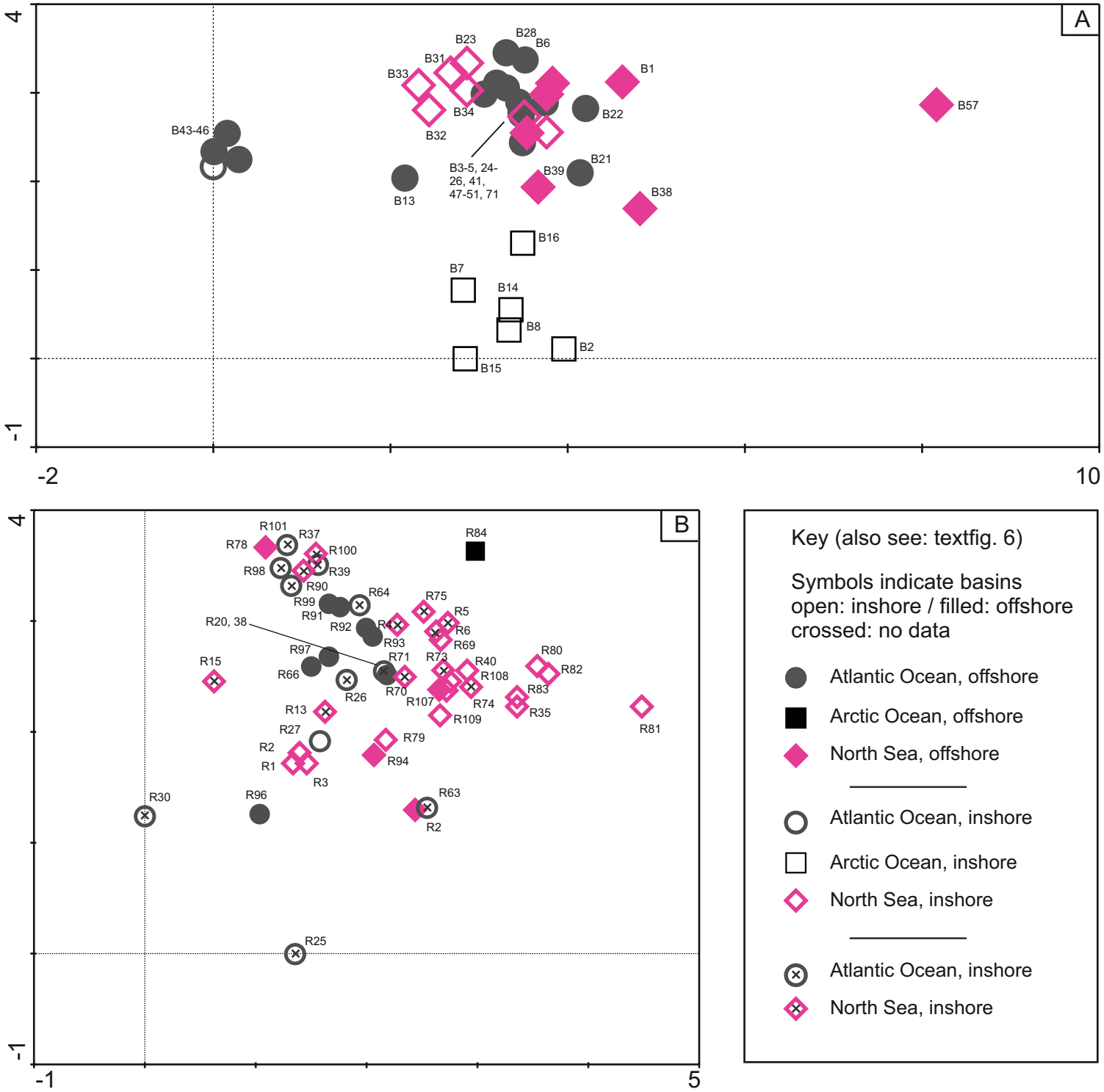
A
4
-1
-2
10
B23
B28
B6
B31
B33
B1
B34
B22
B57
B43-46
B32
B3-5, 24-26, 41, 47-51, 71
B21
B39
B13
B38
B16
B7
B14
B8
B2
B15
B
4
-1
-1
5
R101
R37
R78
R84
R100
R98
R39
R90
R64
R99
R75
R91
R5
R20, 38
R92
R6
R93
R69
R97
R71
R73
R40
R80
R15
R66
R108
R82
R26
R70
R107
R83
R74
R35
R13
R109
R81
R27
R79
R2
R94
R1
R3
R30
R96
R63
R2
R25
Key (also see: textfig. 6)
Symbols indicate basins
open: inshore / filled: offshore
crossed: no data
Atlantic Ocean, offshore
Arctic Ocean, offshore
North Sea, offshore
Atlantic Ocean, inshore
Arctic Ocean, inshore
North Sea, inshore
Atlantic Ocean, inshore
North Sea, inshore

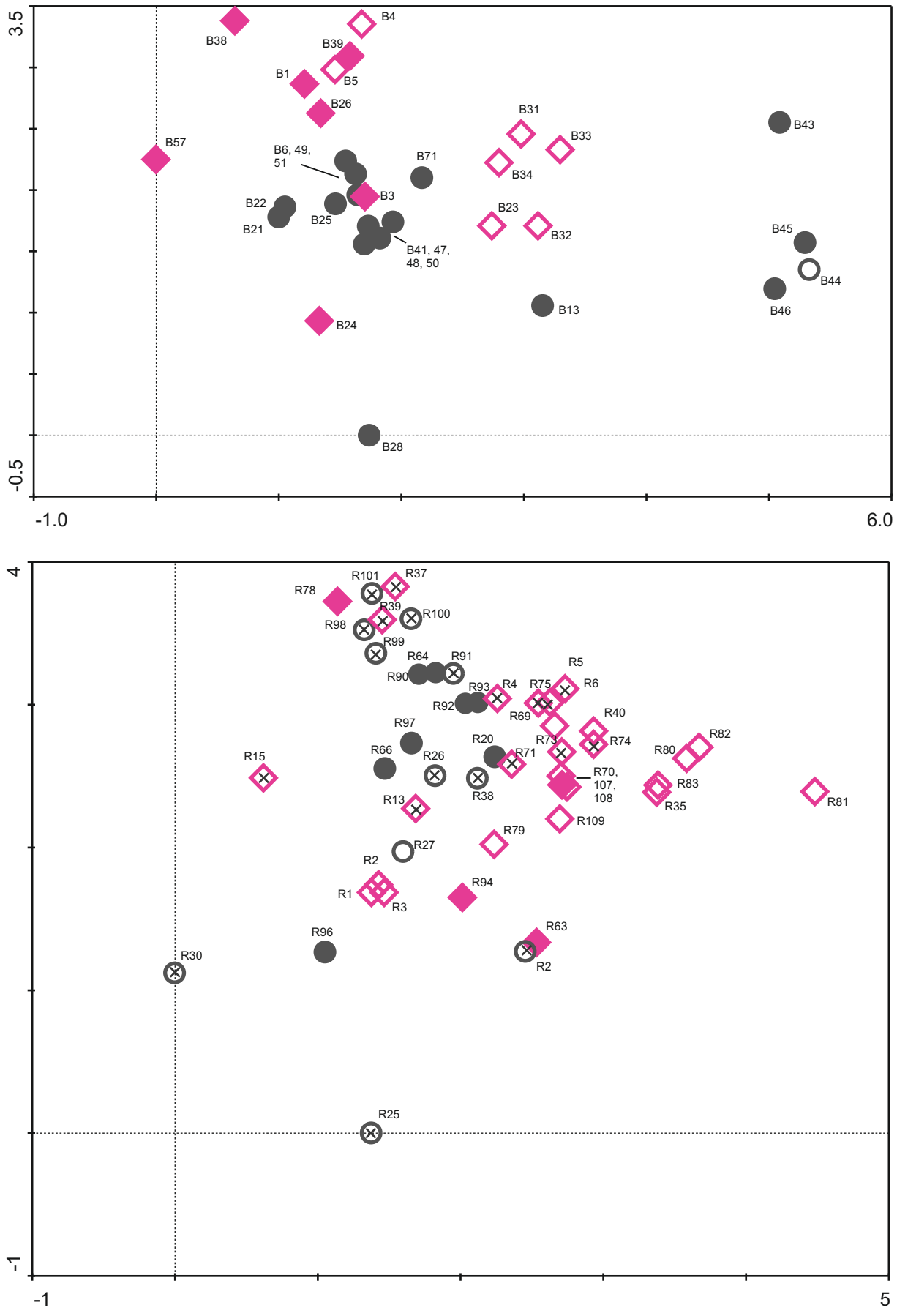


Key (also see: textfig. 6)

Symbols indicate basins; open: inshore / filled: offshore / crossed: no data

| | | |
|---|---|---|
| Atlantic Ocean, offshore | Atlantic Ocean, inshore | Atlantic Ocean, no data |
| North Sea, offshore | North Sea, inshore | North Sea, no data |